

Publisher source acknowledgment:

<https://www.sciencedirect.com/science/article/pii/S0968089619314749> (final version)

DOI: 10.1016/j.bmc.2019.115257

VIRTUAL SCREENING IDENTIFICATION AND CHEMICAL OPTIMIZATION OF SUBSTITUTED 2-ARYLBENZIMIDAZOLES AS NEW NON-ZINC-BINDING MMP-2 INHIBITORS

Antonio Laghezza^{b§}, Grazia Luisi^{a§}, Alessia Caradonna^b, Antonella Di Pizio^{a1}, Luca Piemontese^b, Fulvio Loiodice^b, Mariangela Agamennone^{a*}, Paolo Tortorella^{b*}

^aDepartment of Pharmacy, "G. d'Annunzio" University of Chieti-Pescara, Chieti, Italy

^bDepartment of Pharmacy and Pharmaceutical Sciences, "A. Moro" University of Bari, Bari, Italy

¹Present address: Section In Silico Biology & Machine Learning, Leibniz-Institute for Food Systems Biology at the Technical University of Munich, Freising, Germany

* Corresponding Authors

E-mail address: m.agamennone@unich.it (M. Agamennone), paolo.tortorella@uniba.it (P. Tortorella)

Abstract

Matrix metalloproteinases (MMPs) are a large family of zinc-dependent endoproteases known to exert multiple regulatory roles in tumor progression and invasiveness. This encouraged over the years the approach of MMP, and particularly MMP-2, targeting for anticancer treatment. Early generations of MMP inhibitors, based on aspecific zinc binding groups (ZBGs) assembled on (pseudo)peptide scaffolds, have been discontinued due to the clinical emergence of toxicity and further drawbacks, giving the way to inhibitors with alternative zinc-chelator moieties or not binding the catalytic zinc ion.

In the present paper, we continue the search for new non-zinc binding MMP-2 inhibitors: exploiting previously identified compounds, a virtual screening (VS) campaign was carried out and led to the identification of a new class of ligands. The structure-activity relationship (SAR) of the benzimidazole

scaffold was explored by synthesis of several analogues whose inhibition activity was tested with enzyme inhibition assays. By performing the molecular simplification approach, we disclosed different sets of single-digit micromolar inhibitors of MMP-2, with up to a ten-fold increase in inhibitory activity and ameliorated selectivity towards off-target MMP-8, compared to selected lead compound. Molecular dynamics calculations conducted on complexes of MMP-2 with docked privileged structures confirmed that analyzed inhibitors avoid targeting the zinc ion and dip inside the S1' pocket. Present results provide a further enrichment of our insights for the design of novel MMP-2 selective inhibitors.

Keywords: cancer; matrix metalloproteases; MMP-2; selectivity; non-zinc-binding inhibitors; arylbenzimidazoles.

1. Introduction

Cancer remains a leading cause of morbidity and mortality worldwide, despite the outstanding progress in diagnosis and clinical protocols for treatment. Metastatic tumors, in particular, are highly incurable and account for about 90% of fatalities in oncologic patients [1].

Tumor cell dissemination at distant sites is a complex, multistep process, concisely characterized by tissue invasion, pervasive angiogenesis and avoidance of immune and/or apoptotic destruction. The ability of malignant cells to intravasate into blood and lymphatic vessels, and then to extravasate into the target tissues, implies the demolition of the main physiological barrier to metastasis, namely the extracellular matrix (ECM), a dynamic macromolecular structure which, providing both mechanical and functional sustain to the intracellular spaces, exerts a fine control on cell growth, migration and differentiation, and tissue plasticity [2].

It is not surprising, then, that an ongoing attention is focused on matrix metalloproteinases (MMPs), since members of this multifunctional family of calcium- and zinc-dependent ECM disrupting endopeptidases, have been long recognized as major players in tumor genesis and aggressiveness [3].

As deputed executors of the proteolytic degradation of ECM components (collagen, gelatin, elastin, fibronectin, and proteoglycans) and non-ECM substrates (growth factors, chemokines and cytokines), MMPs are involved in several physiological processes. To avoid excessive tissue degradation, MMP expression and proteolytic activity are finely regulated at the gene transcriptional level and through zymogen activation and inhibition by endogenous modulators (TIMPs, α 2-macroglobulin, and endostatin).

Although the mechanisms mediating dysregulation of these proteases remain unclear, it is widely accepted that abnormal MMP expression and/or activity is strongly implied in the development and progression of metastatic cancer, [4] as well as autoimmune, chronic- [5] and neuro-inflammatory syndromes [6], cardiovascular pathologies [7], viral and bacterial infections, and neurological disorders [8], among all Alzheimer's disease [9].

As a result, the recognition of MMPs as highly attractive targets for anti-cancer intervention has produced an outstanding advance in the comprehension of their structural, mechanistic, and functional roles, in an effort to assist the design of synthetic inhibitors tailored for these peptidases [10].

Currently, 28 isoforms of MMPs have been identified in mammals as mainly secreted and membrane-anchored enzymes, and they have been classified into sub-families according to their substrate specificity, primary structures and cellular localization.

Humans express 23 MMPs, with no fewer than 14 found in the vasculature. The most commonly dysregulated isoforms in cancer, highly correlated to metastatic potential, are the 72 kDa MMP-2 and the 92 kDa MMP-9 (type IV collagenases or gelatinases A and B, respectively), which therefore represent validated goals for therapeutic purposes as well as prospective biomarkers for specific tumors. Because of its involvement in the breast-to-bone metastatic cascade [11], MMP-2 keeps on being the most attractive target for inhibition.

Despite wide substrate variability, MMPs display a high degree of structural homology, in particular for the catalytic domain, containing one functional zinc. The main structural difference between the family members regards the hydrophobic S1' cavity and its surrounding ω -loop that, showing variability in shape, amino acid sequence, and dynamic behavior, represents the major determinant for MMP substrate recognition and selective binding to potential inhibitors [12, 13].

The tight requirement of the zinc ion for catalysis and the presence of diverse substrate binding subsites in the protein have been exploited for the design of the first generations of MMP inhibitors (MMPIs), which are invariantly built up by coupling a substrate- or structure-based peptide-to-peptidomimetic backbone to a metal-chelating moiety, the so-called zinc-binding group (ZBG).

Although most of the ZBG-featuring MMPIs result extremely potent *in vitro*, their application in the oncologic field has been disappointing to date, essentially due to an intrinsic lack of selectivity towards those individual MMPs promoting cancer progression, leading to a loss of the protective effects of others MMPs in tumor stages, as well as to the beneficial role of MMPs and generic metalloproteases in connective tissue homeostasis [14-17].

As a consequence of their poor selectivity profile, most MMPIs produce dose-limiting toxicity, which manifests mainly as the musculoskeletal syndrome (MSS) [18]. Further reasons are implied in the marketing failure of these broad-spectrum inhibitors, including the fact that the clinical trials are performed on patients with terminal-phase cancer, when inhibitors efficacy is reduced owing to several overlapping pathways [19] the scarce tolerability and, particularly for MMPIs of the hydroxamate-type, poor oral bioavailability [20] and loss of efficacy due to metabolic rearrangement of the NH-OH chelating moiety.

To address these shortcomings, two main approaches have been followed in the search for more selective MMPIs, characterized in addition by greater oral bioavailability and improved pharmacokinetic profiles [21]: 1) the introduction of alternative ZBGs [22-26]; 2) the identification of a new class of ligands that, by lacking the ZBG, are not able to bind the metal site. These latter were designed to take

advantage of the steric limitations of the S1' specificity pocket to exploit new productive interactions for selectivity. These inhibitors, identified for MMP-13 [27-32], MMP-8 [33] and MMP-12 [34], which share high S1' conformational flexibility [35], were shown to be equally potent to broad-spectrum MMPs, but much more selective.

The challenge of tuning the activity of disease-related MMPs by exploiting the poorly investigated interactions in the S1' site has led our group to carry on a virtual screening-based project to identify novel non-zinc binding inhibitors (NZBIs) targeting gelatinase A, *i.e.*, MMP-2 [36-39].

Our studies moved from the unprecedented observation that the S1' binding pattern to a non-zinc chelating inhibitor by MMP-8 is mostly conserved in the corresponding MMP-2/ligand complex. This despite the fact that the shorter MMP-2 S1' loop is unable to give the same conformational changes induced, upon binding, at the bottom of the S1' pockets in the MMP-8 and -13 isoforms, which are thought to be crucial for efficient and selective inhibition [36, 38].

Starting from this probe, and guided by an integrated pharmacophore-docking based screening, we previously identified micromolar inhibitors of MMP-2 belonging to the hydroxynaphthyridine and hydroxyquinoline classes. Notably the docked derivatives were not found to bind the catalytic zinc [36]. Hence, the identified structures were submitted to a simplification study in order to disclose the structural determinants for MMP-2 inhibition [38].

The relevance of the subject and the great potential connected to the identification on NZB MMP-2 inhibitors prompted us to go on with the project. Therefore, we decided to exploit previously obtained results to setup a new virtual screening workflow aimed to optimize the search for new and selective non-zinc binding MMP-2 inhibitors. Analogue testing and following synthesis confirmed the prospective role of the benzimidazole scaffold to develop NZBIs of MMP-2.

2. Results and discussion

2.1 Virtual screening

As already stated, the design of NZBIs represents an effective strategy to identify useful MMPs. However, just a few MMP-2 inhibitors not binding the zinc ion have been disclosed so far, therefore, a hierarchical virtual screening (VS) workflow has been setup exploiting previously obtained data about NZBIs, in particular, considering the active compounds obtained in the first VS campaign and the synthesized analogues.

610,000 molecules from Asinex were filtered to eliminate unsuitable compounds by applying the REOS filter [40]; the 3D structures, stereoisomers, tautomers and protomers of the filtered library (490,000 compounds) were generated obtaining almost 1,300,000 resulting structures that were aligned to the pharmacophore hypothesis obtained as described thereafter.

A ligand-based pharmacophore model was generated taking into account the common structural features of the fifteen active compounds previously identified (Table S1 of Supporting Information) [36, 38]. The best pharmacophore hypothesis was composed of five features ADDRR mapping the two aromatic functions (R), the acceptor (A) on the ureic CO group and the two hydrogen-bond donor NH of the urea (D) (**Figure 1**). The obtained hypothesis showed a very good ability to discriminate among active and inactive compounds (BEDROC - Boltzmann-Enhanced Discrimination of Receiver Operating Characteristic = 1, PhaseScore = 1.6). This hypothesis was used to screen the previously mentioned library, saving compounds that map at least 3 out of 5 features.

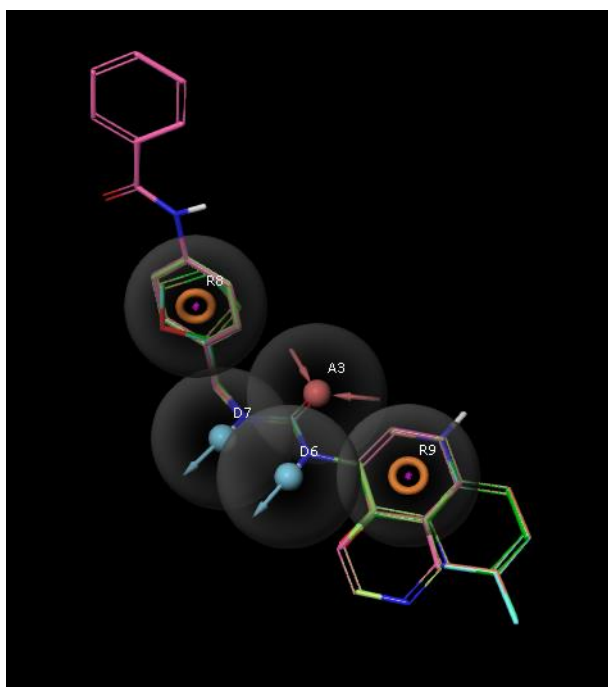


Figure 1. Pharmacophore hypothesis obtained by aligning the already identified NZBIs of MMP-2. Structure of the compounds aligned to the pharmacophore hypothesis is represented as stick (N, O and H are colored on the basis of the atom type, while carbon atoms are colored on the basis of the entry). The hypothesis is composed by five features: 1 hydrogen bond (HB) acceptor (red sphere with arrows), 2 HB donors (cyan sphere with arrow), 2 aromatic rings (orange donuts).

The top 2,000 compounds with highest fitness values were submitted to docking simulations, following a protocol already applied for the rationalization of previously studied inhibitors [38]. Visual inspection of best ranked compounds brought to the selection of 20 virtual hits (Table S2 of Supporting

Information), taking into account the structural diversity and the presence of an aromatic function interacting with the His201 imidazole ring (MMP-2 numbering). These compounds have been purchased and submitted to the following biological evaluation.

2.2. Enzyme inhibition assays

The inhibitory activity of selected hits was evaluated *in vitro* by fluorometric assays using the commercially available catalytic domain of MMP-2, -8, -9 and -13. A preliminary screening was conducted on MMP-2, calculating the percentage of inhibition at 100 μM (**Figure 2**). IC_{50} values were then measured only for compounds showing the highest inhibition.

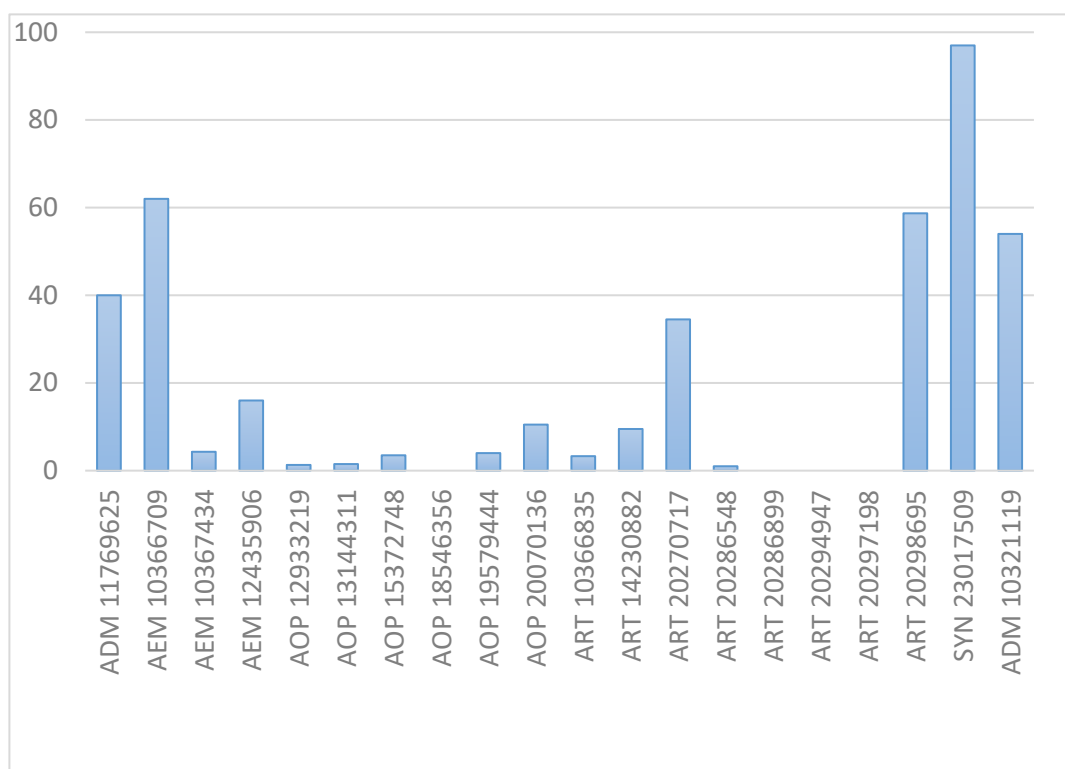


Figure 2. Percentage of inhibition of MMP-2 catalytic domain measured at 100 μM of inhibitor concentration. Tested compounds are reported with their supplier code (**Table 2** of Supporting Information).

The new virtual screening run afforded one hit SYN 23017509 (**1**), structurally different from the previously identified compounds, and with a micromolar activity against MMP-2 and MMP-13 ($\text{IC}_{50}=72 \pm 2$ and $93 \pm 1 \mu\text{M}$, respectively), while it resulted inactive against MMP-8. This compound represents the first example of benzimidazole-based non-zinc binding MMP-2 inhibitor.

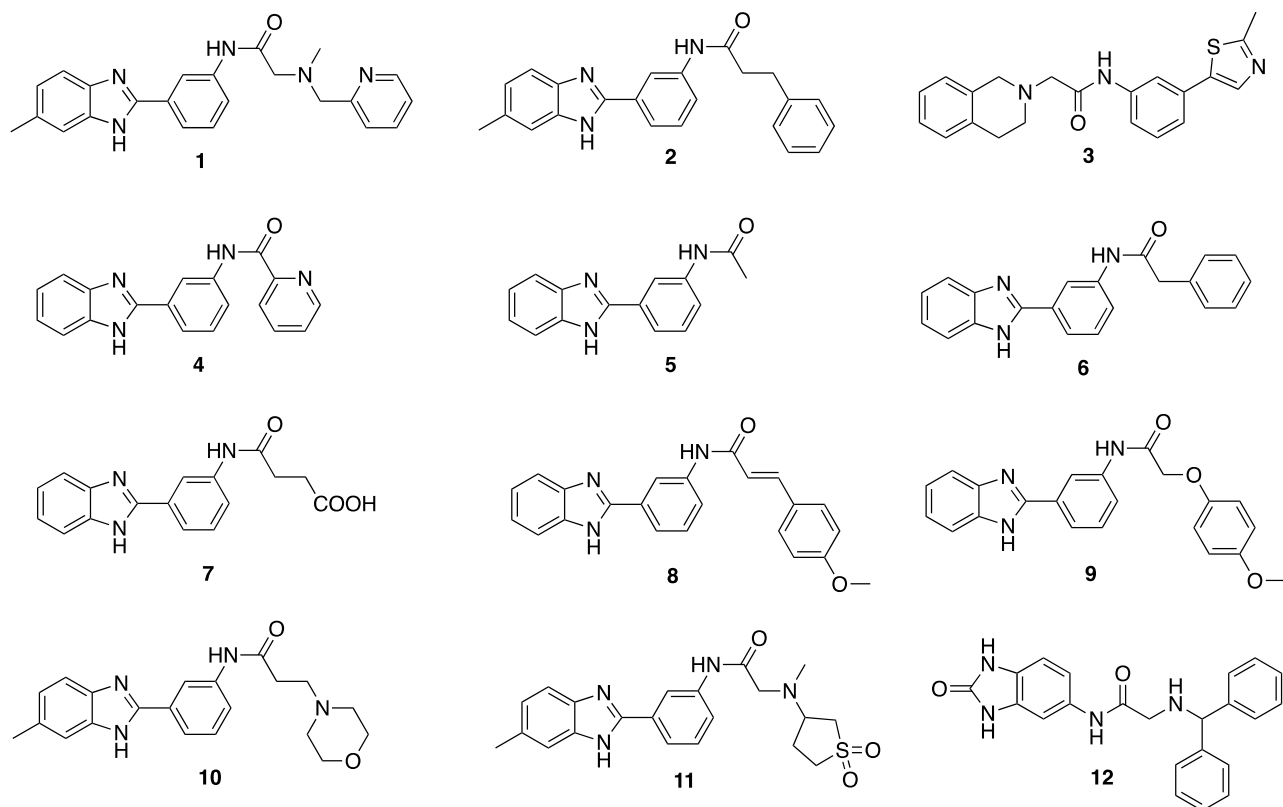


Figure 3. Structure of **1** analogues selected for enzyme inhibition assays.

2.3. Compound 1 series confirmation

To verify the validity of the identified scaffold, a substructure search in the Asinex library was carried out considering the benzimidazole fragment as the scaffold and 11 analogues (**2-12**) were selected and purchased for further testing (**Figure 3**).

The inhibitory activity of **1** analogues was evaluated measuring the percentage of enzyme inhibition at 100 μM toward MMP-2, -8, -9, and -13. The IC_{50} values have been measured only for compounds **2** and **8** that showed the highest percentage of inhibition (all the other compounds presented a negligible inhibition at 100 μM). Obtained data have confirmed the role of benzimidazole scaffold for bioactivity as **2** and **8** have shown an even better inhibition in comparison to **1**; in particular, **2** displayed good activity against MMP-2, and MMP-8, and -9, while it resulted inactive against MMP-13, while **8** confirms the interesting inhibitory profile of **1** sparing the off-target isoform MMP-8 and slightly increasing the potency toward MMP-2 and MMP-13; however, **8** was found devoid of activity towards MMP-9 (**Table 1**). Based on these preliminary activity results, and taking into account the major

chemical versatility for SAR elucidation of compound **2**, and particularly its C ring side chain (see below), compared to **8**, our family of congeners was built up starting from inhibitor **2**.

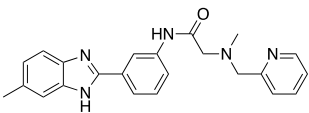
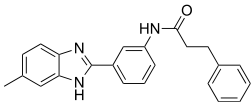
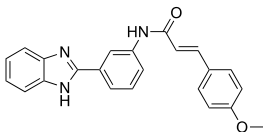
Compound	IC ₅₀ μM			
	MMP-2	MMP-8	MMP-9	MMP-13
1 	72 ± 2	>100	>100	93 ± 1
2 	31 ± 5.3	32 ± 4	26.6 ± 2.3	> 100
8 	48 ± 2	>100	>100	52 ± 7

Table 1. MMP enzyme inhibition data measured for most active benzimidazole analogues.

2.4. Hit optimization

On the basis of these evidences, to have a detailed SAR for this class of inhibitors, we planned to synthesize derivatives of **2** exploring: i) the substitution on the benzimidazole ring A; ii) the nature and position of the substituent on the central phenyl nucleus (C); iii) the substitution of the benzimidazole nucleus with benzoxazole and benzothiazole; iv) the replacement of the phenyl ring (C) with a furan (**Figure 4**).

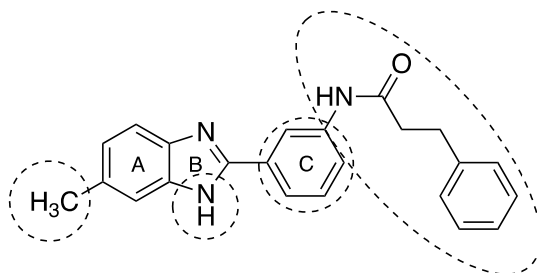


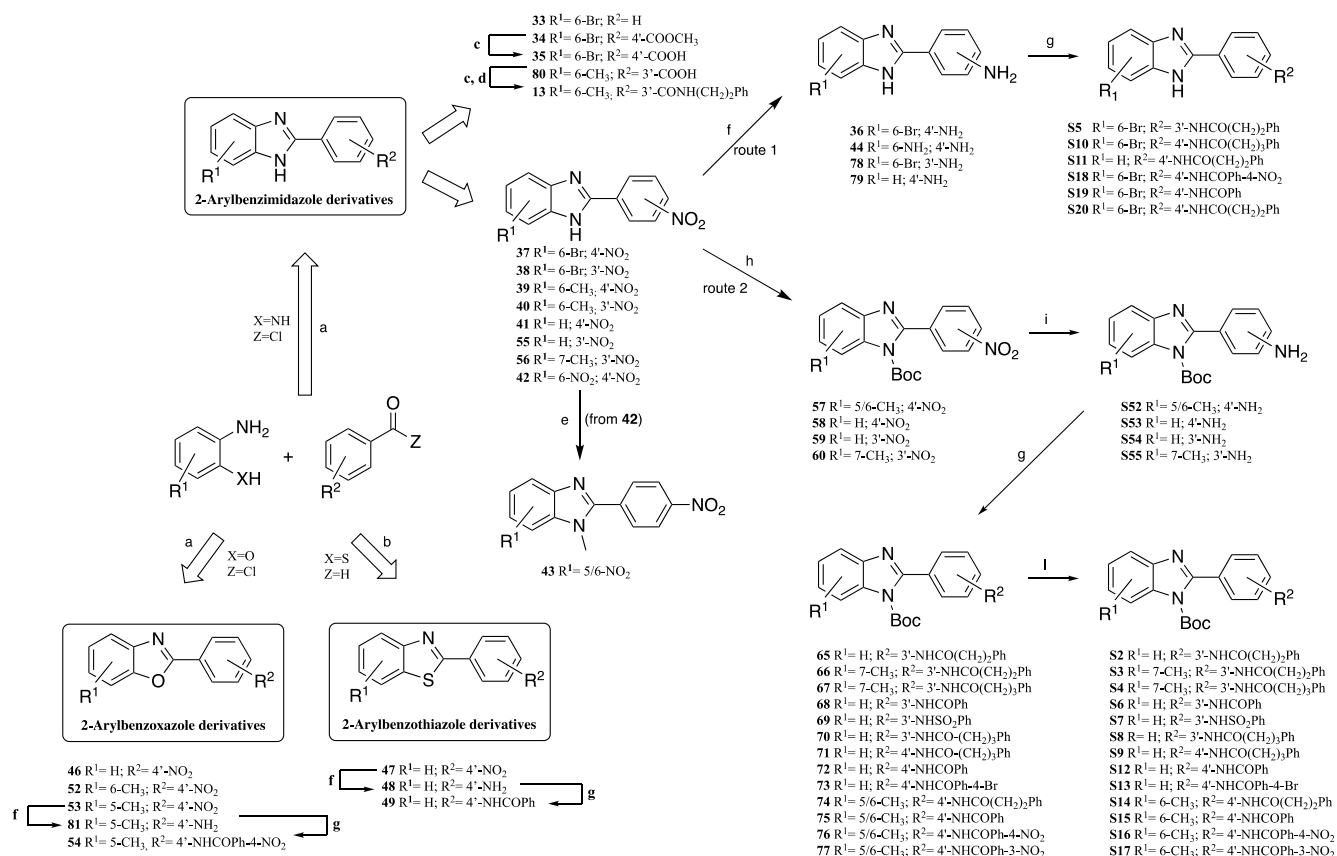
Figure 4. Structural modifications realized on **2** moieties.

Chemistry

Synthesis of 2-arylbenzimidazole, 2-arylbenzoxazole and 2-arylbenzothiazole derivatives

Synthesis of *N*-(benzothiazol-2-yl)-4-nitrobenzamides

Commercially available 1,2-diaminobenzenes were acylated with opportune acyl chlorides and then easily cyclized under acid conditions to the corresponding 2-arylbenzimidazoles **33**, **34**, **37-42**, **55** and **56** (Scheme 1).



Scheme 1. Reagents and conditions: a) *i.* pyridine, reflux, overnight; *ii.* *p*-TsA, xylene, reflux, overnight; b) DMSO, reflux, 1h; c) 1N NaOH, THF, rt, 4h; d) EDC, NEt₃, 2-phenylethylamine, dry DMF, N₂, rt, 22h; e) CH₃I, K₂CO₃, dry DMF, overnight; f) Fe, 6N HCl, EtOH, reflux, 3-5h; g) NEt₃, RCOCl or Ph-SO₂Cl, dry THF, rt, N₂, 3-12h; h) Cs₂CO₃, (*t*-Boc)₂O, MeCN, rt, 4-12h; i) H₂, 5 or 10% Pd/C, EtOH/EtOAc, 3 bar, rt, 12-24h; l) TFA, dry DCM, rt, 2-12h; i)

Depending on R² substitution, the 2-arylbenzimidazole series was split into not-nitrated (**33-35**, **80**, and **13**) and nitrated compounds (**37-42**, **55**, and **56**).

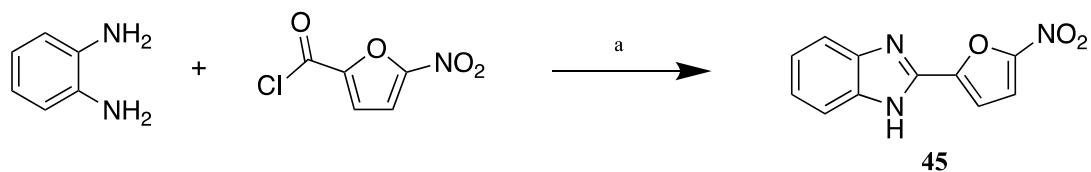
The small group of 2-arylbenzimidazoles with R² ≠ NO₂ included the esters methyl 4'-benzoate (**34**) and its methyl 3'-benzoate analogue, which were subjected to mild alkaline hydrolysis to afford the

corresponding benzoic acid derivatives **35**, as last product, and **80**, respectively. Final condensation of **80** with 2-phenylethylamine in presence of EDC and NEt₃ yielded inverted amide **13**.

On the other side, 2-nitroarylbenzimidazoles **37-42**, **55**, and **56** were the precursors, *via* reduction and subsequent acylation, of the most substantial set of candidates. **42** was also converted into its *N*₁-methylated 2-nitroarylbenzimidazole analog (**43**) by efficient alkylation with CH₃I/K₂CO₃ in dry DMF. Due to the poor stability of bromine atom to catalytic hydrogenation, the reduction of nitro aromatic group for 6-bromo derivatives **37** and **38**, as well as for **41** and **42**, to give the corresponding aniline-derivatives **36**, **78**, **79**, and **44**, was carried out in excellent to acceptable yields by treatment with iron powder in 6N HCl (**Scheme 1**, route 1). Subsequent acylation using the opportune acyl chlorides and NEt₃ in anhydrous THF produced **17**, **22**, **23**, **30-32**. Unfortunately, this procedure gave rise to numerous by-products and the desired compounds were isolated in low yields (16% for **32**). Thus, for the synthesis of remaining derivatives we decided to protect the imidazole nitrogen to avoid its involvement (**Scheme 1**, route 2): *Boc*-protection was quantitatively introduced (**57-60**) and kept all through the sequential steps, *i.e.* catalytic hydrogenation of nitro group to give **61-64**, subsequent acylation with the required acyl chlorides (**65-77**), till the final acidolytic removal, affording the desired *N*-deprotected products **14-16**, **18-21**, **24-29**, with good overall yields.

Benzene substitution of the benzimidazole scaffold gave rise to the 1,3-tautomers which could be seen in some ¹H NMR spectra of the 2-arylbenzimidazole derivatives. Equivalence and fast exchange of the 4,7-protons and 5,6-protons accounted for the broad signals of the aromatic protons in the ¹H NMR spectra [41] On the basis of this evidence, being the position of 4/7 and 5/6 equivalent, the 2-arylbenzimidazole derivatives are shown with the benzene substituents in position 6 and 7. This is not valid for those compounds substituted on the benzimidazole nitrogen, as *N*-methylated **43**, and all *N*-Boc intermediates envisioned in route 2.

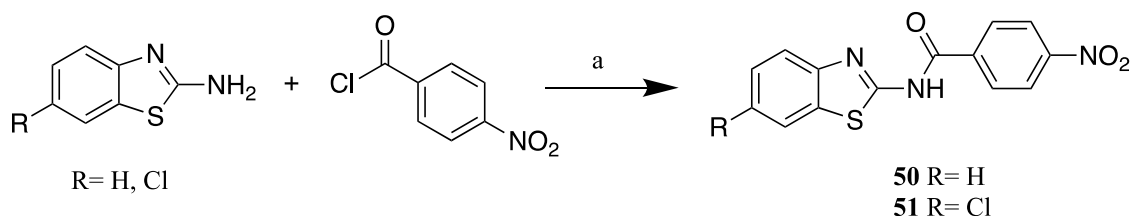
2-(5-Nitrofuran-2-yl)-benzimidazole (**45**) was assembled as described in satisfactory yields and was not further processed; it represents the only benzimidazole to be prepared featuring a furanyl heterocycle as bioisosteric replacement of the 2-phenyl substituent (**Scheme 2**).



Scheme 2. Reagents and conditions: a) *i.* pyridine, reflux, overnight. *ii.* *p*-TsA, xylene, reflux, overnight.

A few benzoxazole and benzothiazole derivatives were considered as isosteric counterparts of the benzimidazole scaffold. Starting from commercially available 2-aminophenols and 4-nitrobenzoyl chloride, 2-(4'-nitroaryl)benzoxazole **46**, **52** and **53** were prepared in the same conditions described for benzimidazoles; 2-(4'-nitroaryl)benzothiazole **47** was instead obtained by refluxing 2-aminothiophenol and 4-nitrobenzaldehyde in DMSO (**Scheme 1**). Owing to the lack of the reactive nitrogen, 2-nitroarylbenzoxazole **53** and 2-nitroarylbenzothiazole **47** were processed to **54** and **49** through aniline intermediates **81** and **48** by following route 1 conditions, *i.e.* iron-mediated reduction in acidic conditions followed by smooth acylation.

In order to evaluate whether the phenyl appendage needed to be directly linked, *via* a C-C bond, to the 2-position of the heteroaromatic nucleus for the inhibitory activity, or some fragment was tolerated between the two rings, compounds **50** and **51**, containing an interposed NHCO unit, were synthesized in acceptable yields through acylation of corresponding 2-amminobenzothiazoles with *p*-nitrobenzoyl chloride in the presence of NEt₃ in dry THF (**Scheme 3**).



Scheme 3. Reagents and conditions: a) NEt₃, dry THF, rt, 3-12h.

2.5. Biochemical assays and SAR analysis

All synthesized compounds were tested in enzyme inhibition assays against MMP-2, -8, -9 and -13 (**Tables 2-5**) and compared with lead compound **2**. Inhibition on MMP-9 has been evaluated because of its similarity to MMP-2.

Our first SAR investigation regarded those analogues most closely related to **2** in structure and size. Thus, intermediate 2-aminoarylbenzimidazoles **36**, **44**, **78**, **79**, and *N*-(Boc) 2-aminoarylbenzimidazoles **61-64** opened the way to amidated derivatives **14-32** (**Scheme 1**). In order to better explore the importance of nature and position of the substituent on the benzimidazole ring, the methyl group present

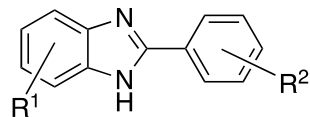
in the 6-position of **2** was replaced with a hydrogen atom (**14**) or moved to the position 7 (**15**). Obtained derivatives were overall less active than **2** against tested MMPs, except for the conserved activity of **15** on MMP-8. A slight improvement in activity was observed after replacement of the methyl residue with a bromine atom (**17** vs **2**) (**Table 2**).

It came to our attention that the 3'-phenylacetamide group in **6** (**Figure 3**) could be elongated of one methylene unit to give inhibitor **14** ($R^1 = H$), with little gain in potency against tested MMPs with respect to **6**. We were then intrigued in investigating the homologation approach for the phenylalkanoylamide chain linked to the C ring, with the following results compared to parent **2** (**Table 2**):

- the addition of a further CH_2 group in the alkanoyl amide appendage positioned in 3' did not alter significantly the inhibitory activity against MMP-2, as shown for the 7-methyl substituted analog **16** in comparison to **15**, although promoted a negligible increase in selectivity towards MMP-2 with regard to MMP-8 ($s = 0.7$ vs. 0.5 , **Table 2**); compound **20** ($R^1 = H$) resulted, however, a more efficient inhibitor than inferior homologue **14** against all MMPs. The opposite was observed by moving the $PhCH_2CH_2CH_2CONH$ chain from the 3'- to the 4'-position of the C ring, exemplified by the sensible drop in activity for inhibitor **21** compared to **23** ($R^1 = H$), as well for the 6-bromine derivative **22** versus **32**; despite this, **21** exhibited an acceptable selectivity towards the target isoform;
- more significantly, the truncation of the phenylpropionamide to the simpler benzamide chain led to a noticeable gain in activity in comparison to **2** and its congeners towards MMP-2 and MMP-13. The effect, which is already evident in the 3'-benzamide derivative **18** ($R^1 = H$, see **14**), is observed also for the 4'-substituted inhibitors **24** ($R^1 = H$, vs **23**) and **27** ($R^1 = 6-CH_3$, see **26**), with the exception of **31** ($R^1 = 6-Br$) which is practically equipotent to **32** on MMP-2. Compounds **24**, **27**, and **31** are *de facto* the first undersized derivatives exhibiting a one-digit micromolar inhibition on both targets, and emerging selectivities, particularly **31** ($s = 7.8$). Compound **18** well exemplifies the tolerance to bioisosteric replacement in different parts of the amide chain linked to the C ring; in fact, it represents the efficient carba-analog of the pyridine-containing inhibitor **4** (**Figure 3**), which was found practically devoid of activity against the whole MMP spectrum; this could be in relation to the higher electron density of the pyridine nucleus compared to the **18** phenyl ring. Secondly, **18** amide bond was replaced with a sulfonamide junction, known to introduce electronic and geometrical properties which may be peculiar to recognition and binding: the resulting surrogate **19** was found a weaker inhibitor towards MMP-2 and MMP-13 with respect to its amide counterpart,

thus evidencing the critical queries for binding affinity. Once the aryl-spacer length required for optimal activity was settled, we explored the effect of the substitution on the distal aromatic ring: curiously, the addition of a bromine atom in the 4-position resulted in a slightly less efficient inhibitor (**25** compared to **24**), while the introduction of the likewise electron-withdrawing nitro group in 4- (**28** and **30**) or 3-position (**29**) afforded an approximate two-fold increase in activity compared to unsubstituted **27** and **31**, and resulted in remarkably potent inhibition against MMP-2 and MMP-13 (IC_{50} values of $3.3\pm 0.4/1.8\pm 0.4$, $3.1\pm 0.3/3.9\pm 1.6$, and $3.9\pm 0.9/2.2\pm 0.2$ μM , respectively), with **28** and **29** featuring good selectivity. It is interesting to note that benzimidazole derivatives **28-30** exhibit equal ligand efficiency (LE) values (0.27).

Table 2. *In vitro* inhibitory activity, selectivity and ligand efficiencies for benzimidazole derivatives **13-32** compared to lead molecule **2**, evaluated by fluorometric assay using commercially available catalytic domain of MMP-2, -8, -9 and -13. IC₅₀ μM values are reported as the mean ± SEM of at least 2 independent experiments performed in triplicate.



Compd	R ¹	R ²	MMP-2	MMP-8	MMP-9	MMP-13	MMP-8/ MMP-2	LE MMP-2*	LLE MMP-2*
2	6-CH ₃	3'-NHCOCH ₂ CH ₂ Ph	31±5	32±4	26.6±2.3	>100	1.0	0.23	-0.80
13	6-CH ₃	3'-CONHCH ₂ CH ₂ Ph	45±5	40±2	37.7±1.5	>100	0.9	0.22	-0.54
14	H	3'-NHCOCH ₂ CH ₂ Ph	87±26	41.9±1.4	68±27	>100	0.5	0.21	-0.74
15	7-CH ₃	3'-NHCOCH ₂ CH ₂ Ph	64±18	29±6	60±29	>100	0.5	0.21	-1.12
16	7-CH ₃	3'-NHCOCH ₂ CH ₂ CH ₂ Ph	60±2.5	40.9±0.4	38.6±2.8	91±56	0.7	0.21	-1.54
17	6-Br	3'-NHCOCH ₂ CH ₂ Ph	16 ±1	12.5 ±1.5	14.5±0.5	73±5	0.8	0.24	-0.77
18	H	3'-NHCOPh	11.9±2.7	46±16	57±6	35±15	3.9	0.28	0.54
19	H	3'-NHCO ₂ Ph	65.4±3.0	43.2±1.4	36±9	94±13	0.7	0.23	0.41
20	H	3'-NHCOCH ₂ CH ₂ CH ₂ Ph	47±7	34.6±2.6	43±12	81.2±1.3	0.7	0.22	-0.92
21	H	4'-NHCOCH ₂ CH ₂ CH ₂ Ph	96±36	>100	>100	50±3	>1.0	0.20	-1.23
22	6-Br	4'-NHCOCH ₂ CH ₂ CH ₂ Ph	31±1	67±1.8	58.0±2.5	22.2±2.0	2.2	0.22	-1.50
23	H	4'-NHCOCH ₂ CH ₂ Ph	19±3	64±6	29±9	15.2±0.3	3.4	0.25	-0.08
24	H	4'-NHCOPh	6.5±2.5	28±17	16±10	7.5±2.5	4.3	0.30	0.81
25	H	4'-NHCO-Ph-4-Br	9.4 ± 1.5	55 ± 1	41±16	10.9±1.2	5.9	0.28	-0.11
26	6-CH ₃	4'-NHCOCH ₂ CH ₂ Ph	25.3±1.0	77±7	60±9	17.9±2.3	3.0	0.23	-0.71
27	6-CH ₃	4'-NHCO-Ph	8.6±0.7	45.3±0.7	28.4±2.5	6.5±0.6	5.3	0.28	0.18
28	6-CH ₃	4'-NHCOPh-4-NO ₂	3.3± 0.4	25.5±1.0	10.7±0.5	1.8±0.4	7.7	0.27	0.65
29	6-CH ₃	4'-NHCOPh-3-NO ₂	3.9±0.9	20.9±2.9	14.5±1.4	2.2±0.2	5.4	0.27	0.58

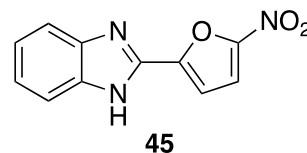
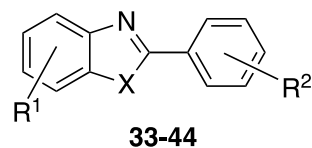
30	6-Br	4'-NHCOPh-4-NO ₂	3.1±0.3	7.9±2.8	6.4 ±1.1	3.9±1.6	2.6	0.27	0.43
31	6-Br	4'-NHCOPh	6.42±0.29	50±2	32 ±1.9	3.9±1.6	7.8	0.28	0.05
32	6-Br	4'-NHCOCH ₂ CH ₂ Ph	7.0±0.1	8±1	11.5±1.5	6.5±1.5	1.1	0.26	-0.42

*LE: the ligand efficiency of compounds was calculated by converting in ΔG the IC₅₀ value toward MMP-2 and then dividing the obtained value by the number of ligand heavy atoms [42].

**LLE: lipophilic ligand efficiency was calculated by subtracting the LE to the calculated logP value [43].

Based on these initial results, the effective weight of the phenylalkanoylamide chain in improving the interactions network inside the enzymatic cleft remained to be established; thus, the molecular simplification strategy was carried to the utmost extremes, with the investigation of simpler arylbenzimidazoles lacking this appendage; this further set comprised most of intermediates in the chemical routes to our bulkier inhibitors, with some newly synthesized compound (**Scheme 1**); here the importance of small R² substituents directly linked to the C aromatic ring was ascertained (inhibitors **33-44**, **Table 3**).

Table 3. *In vitro* inhibitory activity, selectivity and ligand efficiencies for benzimidazole derivatives **33-45** evaluated by fluorometric assay using commercially available catalytic domain of MMP-2, -8, -9 and -13. IC₅₀ μM values are reported as the mean ± SEM of at least 2 independent experiments performed in triplicate.



Compd	R ¹	R ²	X	MMP-2	MMP-8	MMP-9	MMP-13	MMP-8/ MMP-2	LE MMP-2	LLE MMP-2
33	6-Br	H	NH	>100	>100	>100	>100	-	-	-
34	6-Br	4'-COOCH ₃	NH	9.0±3	26.3±1.4	20.7±1.2	19±8.6	2.9	0.35	0.99
35	6-Br	4'-COOH	NH	31.5 ±1.5	35±7	27±4	43±5	1.1	0.33	1.95
36	6-Br	4'-NH ₂	NH	10.0±1.5	26.0±2.5	21.7±2.0	21±4	2.6	0.40	1.78
37	6-Br	4'-NO ₂	NH	8.8±0.8	10±4	10±0.1	10.5±2.5	1.1	0.37	1.07
38	6-Br	3'-NO ₂	NH	>100	>100	>100	47±4	-	-	-
39	6-CH ₃	4'-NO ₂	NH	6.5±0.7	23±12	22±6	6.1±0.1	3.5	0.37	1.45
40	6-CH ₃	3'-NO ₂	NH	14±3.9	27±14.4	36.6±0.1	15.5±2.4	1.9	0.35	1.11
41	H	4'-NO ₂	NH	82±5	64±4	56.5±0.5	>100	0.8	0.31	0.87
42	6-NO ₂	4'-NO ₂	NH	4.2±0.2	25±10	23.3±10.5	12±7	6.0	0.35	2.22
43	5/6-NO ₂	4'-NO ₂	NCH ₃	18±12	>100	>100	14±9	>5.6	0.30	1.35
44	6-NH ₂	4'-NH ₂	NH	>100	>100	>100	>100	-	-	-
45				31±7	27±5	32±4	33±4	0.9	0.36	2.14

Although the unsubstituted derivative **33** ($R^2 = H$) was found inactive against all the MMPs under scrutiny, R^2 replacement with a 4'-positioned acid group (**35**) led to no perturbing effects compared to **2**, and rather introduced inhibitory activity against MMP-13. The substitution with an ester (**34**) or amine group (**36**) in 4' even led to a meaningful increase of the inhibitory activity towards the target isozyme MMP-2, and to an appreciable MMP-13 inhibition, compared to the lead compound. Out of the context of R^2 simplification but following this outcome, we considered **80**, a 3'-carboxy analogue of **35**, for amidation with 2-phenylethylamine, just to explore the amide inversion approach referred to **2** (**Scheme 1**). Unfortunately, the inverso-isomer at the NHCO junction **13** (**Table 2**) resulted a weaker inhibitor towards the whole panel of MMPs, compared to the prototype.

The introduction of a nitro group in 4'-position provided the extremely efficient inhibitors **37** and **39**, each approximately equipotent towards MMP-2 and MMP-13 ($IC_{50} = 8.8 \pm 0.8 / 10.5 \pm 2.5 \mu M$, and $6.5 \pm 0.7 / 6.1 \pm 0.1 \mu M$, respectively), whereas the positioning of the same group in 3' determined a loss of the inhibitory potency against all tested MMPs, more relevant for the 6-bromine derivative **38** (see **37**) with respect to the 6- CH_3 -substituted inhibitor **40** (*vs.* **39**). The presence of two nitro groups, in both 6- and 4'-positions (**42**), further increased the inhibitory activity against MMP-2 ($IC_{50} = 4.2 \pm 0.2 \mu M$). It is interesting to note that efficient inhibitors **36**, **37**, and **39** exhibit the highest values of LE (LE values of 0.40, 0.37, and 0.37, respectively); they all share a small 4- NO_2 -phenyl (4- NH_2 -phenyl for inhibitor **36**) appendage directly linked to the benzimidazole nucleus, while in the three most efficient MMP-2 inhibitors (derivatives **28-30**) a further carbamidophenyl moiety is interposed between the NO_2 -phenyl group and the benzimidazole; accordingly they share a far lower LE value (0.27) as to the aforementioned inhibitors.

The reduction of both nitro groups in 6- and 4'-position (**44** *versus* **42**) plainly truncated compound activity. Finally, the methylation of the **42** benzimidazole nitrogen to give product **43** as isomeric mixture led to poorer inhibitory results towards MMP-2, associated with a full loss of activity toward MMP-8 and MMP-9. Hence the importance of having the free NH of benzimidazole moiety, which seems to be involved as hydrogen bond donor (HD) effector in interactions important for the inhibitory activity of related compounds.

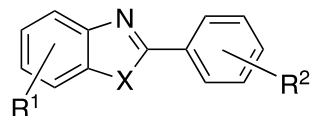
Our further synthetic efforts concerned the replacement of the 4'-activated phenyl ring with the 2-(5-nitrofuranyl) bioisosteric nucleus: the change afforded the good inhibitor **45**, equipotent against the whole MMP panel, which is however superior only to the 4'- NO_2 -substituted arylbenzimidazole **41** ($R^1 = H$) towards MMP-2 and MMP-13 (**Scheme 1**, **Table 3**).

Furthermore, considering the role that the benzimidazole scaffold plays as a structural determinant for binding affinity, we were tempted to investigate the effects of introducing alternative heteroaromatic nuclei by bioisosteric replacement of nitrogen with O/S atoms on inhibitory activity. Thus, we decided to prepare a small series of 2-arylbenzoxazole and 2-arylbenzothiazole derivatives corresponding to the most efficient benzimidazole inhibitors (**Scheme 1**), for comparison of their inhibitory activity against MMP-2, -8, -9 and -13 (**Table 4**). It deserves to be mentioned that the replacement of benzimidazole with benzoxazole and benzothiazole prevents tautomer formation.

In the series of benzamide-linked 2-arylbenzoxazoles, replacing N (**28**) with O (**54**) resulted in an almost five-fold decrease of inhibitory potency towards MMP-2, MMP-8, and MMP-13. For related 2-arylbenzothiazoles, the substitution (**49**) afforded no advantages with respect to the benzimidazole analogue (**24**).

By adopting the fruitful simplification approach, 2-arylbenzoxazoles **46**, **52**, and **53**, and 2-arylbenzothiazole **47** and **48**, were prepared (**Table 4**). Noteworthy was the fact that 2-arylbenzoxazole **46** and 2-arylbenzothiazole **47**, featuring a 4'-nitro substituent as R², resulted more potent than the corresponding benzimidazole analogue **41** towards all MMPs, showing very low micromolar activities against MMP-2 and MMP-13. Compound **52** (R¹ = 6-CH₃) was shown to maintain almost unchanged the inhibitory efficacy of its bioisoster **39**. Shifting the methyl group from the 6- to the 5-position of the benzoxazole nucleus (isomer **53**) had no consequences on activity. In the 2-arylbenzothiazole set, the attempted replacement of the 4'-nitro group with an amino counterpart (**48**) had a detrimental effect on inhibitory behaviour, interesting all MMPs.

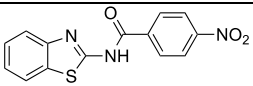
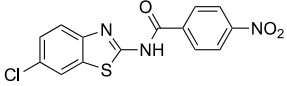
Table 4. *In vitro* inhibitory activity, selectivity and ligand efficiencies for benzimidazole isosteres **46-49** and **52-54** evaluated by fluorometric assay using commercially available catalytic domain of MMP-2, -8, -9 and -13. IC₅₀ μM values are reported as the mean ± SEM of at least 2 independent experiments performed in triplicate.



Compd	R ¹	R ²	X	MMP-2	MMP-8	MMP-9	MMP-13	MMP-8/ MMP-2	LE MMP-2	LLE MMP-2
46	H	4'-NO ₂	O	5.8±0.1	46±2	36±4	7.3±1.8	7.9	0.40	1.96
47	H	4'-NO ₂	S	6.5±1.5	10.5±1.5	11.5±0.5	7.5±0.5	1.6	0.40	1.11
48	H	4'-NH ₂	S	>100	88±0.1	79 ±0.1	>100	-	-	-0.31
49	H	4'-NHCOPh	S	16.4±1.7	38±4	42±1	21±4	2.3	0.27	-0.44
52	6-CH ₃	4'-NO ₂	O	9±1	29 ±16	18±5	9.4±2.4	3.2	0.36	1.21
53	5-CH ₃	4'-NO ₂	O	9.7±2.5	16.4±5.2	14.9±3.5	8.8±2.2	1.7	0.36	1.25
54	5-CH ₃	4'-NHCOPh-4-NO ₂	O	15.9±6.2	14.7±1.7	20±4	11±3	0.9	0.24	-0.09

As final investigation, in the benzothiazole series we examined the effects of removing the C phenyl ring by direct insertion of the 4-nitrobenzamide chain in position 2 of the heteroaromatic scaffold (**Scheme 3** and **Table 5**): the general loss of activity, as compared to **49**, observed for resulting derivatives **50** and **51** (with this latter conserving only a residual activity against MMP-13) would seem to disclose a pivotal role for the central aromatic nucleus in the binding process.

Table 5. *In vitro* inhibitory (expressed as μM IC_{50} values) activity of **50** and **51**.

Compd		MMP-2	MMP-8	MMP-9	MMP-13
50		>100	>100	>100	>100
51		>100	>100	>100	20±0.1

Taken together, these results indicated that the benzoxazole and benzothiazole scaffolds offer advantage in terms of activity with respect to the benzimidazole moiety only in the case of compounds **46** and **47**.

Overall, the following considerations on this new series of compounds can be pointed out:

- 2-Aryl (or heteroaryl)-substituted benzimidazole or related heteroaromatic scaffolds are essential for inhibitory activity.
- Compounds with R^1 and R^2 substituents in position 6 and 4' respectively are better inhibitors against all MMPs under scrutiny, and in particular towards MMP-2, in comparison to positional isomers or unsubstituted analogues.
- As a rule, the presence of electron acceptor groups has favourable effects on the inhibitory potency of derivatives.
- Nitro and bromine are the best R^1 groups in terms of increase of inhibitory activity.
- 3- or 4-nitrobenzamide chain and the nitro group are the preferred substituents in R^2 position.
- Nitro groups in position 6 and 4' result in high activity against MMP-2, which is drastically lowered upon reduction of both substituents.

- Replacement of the benzamide moiety of the side chain with a benzenesulfonamide mimic leads to a decrease in inhibition towards MMP-2 and MMP-13.

In our hit optimization process, the control of candidates' molecular size and lipophilicity was corroborated by Ligand Efficiency (LE), Lipophilic Ligand Efficiency (LLE), and related parameters reported *in extenso* in **Tables 2-4** for the different MMP isoforms under study. In this regard, there is a growing consensus on the reliability of LLE metric for structural and pharmacokinetic drug optimization processes [43].

Starting from the non-zinc-binding MMP inhibitor **2** and its phenylpropionamide-containing congeners, we successfully performed a molecular simplification approach, leading to the selection of different sets of candidates for further progression, with up to a ten-fold increase in MMP-2 inhibitory activity and selectivity towards off-target MMP-8, compared to the lead compound. This is surprising, since quite often the strategy for ligand potency implementation requires an increase in molecular weight to enhance contacts inside the protein; the only oversized **2** analogue displaying single-digit micromolar inhibition against MMP-2 is **32**, but in the case some aspecific hydrophobic effects are thought to play a role in binding affinity, as suggested by the elevated *clogP* value.

The most potent inhibitors **28-30** were obtained through reduction of the phenylpropionamide chain by two methylene units, with an appreciable decrease in lipophilicity compared to **2**; due to substituent optimization, the number of heavy atoms increases in **28-30** but, despite this, ligand efficiencies result higher (LE = 0.27) than that of the lead compound (LE = 0.23). The three benzimidazole derivatives are equipotent against MMP-2 and exhibit equal LE values; it is interesting to note that, although **28** and **29** share the same *clogP* value being 4/3-NO₂ positional isomers, they slightly differ in their lipophilic efficiencies, ranging from LLE = 0.65 for the most selective **28** (*s* = 7.7) to LLE = 0.58 for **29** (*s* = 5.4), thus suggesting for **28** the implication of more specific contacts inside the target cleft. We can tentatively argue that the MMP-2 S1' pocket is more favourably involved, through a suitably oriented charged site, in interactions with a 4- (in spite of 3-) positioned nitro group on the benzamide moiety.

Derivatives **34**, **36**, **37**, **39**, and **42** are among the most potent inhibitors obtained after complete removal of the benzamide appendage linked to the C ring; this change determined a significant drop in molecular weight and lipophilicity, but more importantly the loss of the NHCO polar unit and the related hydrogen donor/acceptor system. Since these compounds are equipotent with analogues **28-30**, it could be proposed that truncation of the benzamide fragment has no effects on the factors driving the affinity

of the ligand for the protein. The privileged structures, featuring the highest LLE and LE values, are represented by **42** (LLE = 2.22, LE = 0.35, $s = 6.0$) and **36** (LLE = 1.78, LE = 0.40). For **36** the reduction in lipophilicity is partly due to the presence of the polar NH₂ substituent, which is most probably solvent-exposed and consequently engaged in interactions unrelated to the identity of the binding site, as supported by its lack of selectivity ($s = 2.6$).

A final set of single-digit micromolar inhibitors of MMP-2 was disclosed by following the bioisosteric replacement approach, which led to benzoxazole (**46**, **52** and **53**) or benzothiazole (**47**) congeners. Particularly arylbenzoxazole **46** deserves to be selected for its properties (LLE = 1.96, LE = 0.40); **46** represents a good inhibitor also in terms of selectivity ($s = 7.9$).

Unfortunately, efforts to reach selectivity towards MMP-2 in relation to the off-target MMP-8 (**Tables 2** and **3**) were disappointing for the new inhibitors. In fact, only eight compounds among all displayed appreciable selectivity, with s values ranging from 7.9 (**46**) to 5.3 (**27**).

2.6. Molecular Modeling

In order to achieve a better understanding of the binding process involving this class of NZBIs, an accurate structure-based study has been carried out by docking all studied compounds in the MMP-2, -8, -9 and -13 binding site. Docking calculations have been carried out using Glide and applying a semi-rigid docking protocol. The benzimidazole scaffold has two possible tautomers and, when substituted, the two forms are equally probable, therefore both have been considered in the docking calculations.

Generally, all compounds occupy the S1' site, as expected, with the central phenyl ring (**Figure 5**) facing the His201 side chain and the benzimidazole occupying the distal portion of the S1' site. A rather well conserved H-bond is formed between the benzimidazole NH and the Ala220 carbonyl oxygen. The amide substituent moves toward the S2' site.

The methyl or Br substituent on the benzimidazole fits in the S1' site improving the hydrophobic interaction. In some case the Br forms a contact with the Thr229 OH, while the methyl has positive contacts with Leu197 and Phe232.

Moving the R² substituent from 3' to 4' does not change activity toward MMP-2 and selectivity substantially; in fact, while 3' amide NH forms a H-bond with Pro221 CO, the amide CO is not able to reach the Leu164 and Ala165 NH. In the 4' substituted compounds the amide CO can form H-bonds with residues on the top of the S1' site.

It is well known that docking calculations are not able to provide a comprehensive picture of the binding process as it neglects the role of water molecules and the flexibility of the system; therefore, Molecular Dynamics (MD) calculations have been carried out for the complexes of MMP-2 with docked poses of **2**, **28** and **42**.

Obtained results confirm that ligands occupy the S1' site and the main interaction involves the His201 imidazole ring. Details about the MD simulations are reported in the SI.

Mostly conserved interactions have been monitored during the simulation and those retrieved in more than the 30% of saved frames are reported in **Figure 5**.

For the ligand **2** the docked binding geometry is almost conserved with the π - π stacking with His201 side chain and the H-bond between the benzimidazole NH and the Ala220 CO as the most stable. The phenylpropionamide portion is solvent exposed and moves toward the S2' site but does not form any specific interaction, as resulting from the RMSF graph.

Ligand **28**, that presents a 4'substitution on the central phenyl ring, quickly reaches a stable binding conformation. In fact, it shifts toward the bottom of the S1' site forming a cation- π interaction with the Arg233 side chain and allowing the NO₂ substituent to interact with His201 and Glu202 via a water molecule. The benzimidazole ring loses its H-bond interaction but the amide NH is bound to Gly216 CO through a water molecule.

Ligand **42** maintains its binding mode for a half of the simulation, largely changing its starting position in the last 9 ns of simulation. The ligand moves slightly toward the distal portion of the S1' site with the nitro-substituents providing interactions with Glu202 and Ala165 mediated by water molecules, the phenyl ring forms two π -stacking interactions with His201 and Tyr223 side chains, while the benzimidazole NH is H-bonded to Ala220 and Ile222. The benzimidazole NO₂ substituent forms productive contact with Arg233 and Thr229 OH at the bottom of the S1' site.

Summarizing, **42** results the most promising starting point for a new series of ligands as its binding mode demonstrates the role of key interactions between the arylbenzimidazole scaffold and the S1' site of MMP-2.

MD simulations, moreover, demonstrate that these ligands are not able to bind the catalytic zinc ion suggesting the possibility to exploit the S1' site to obtain selective binders.

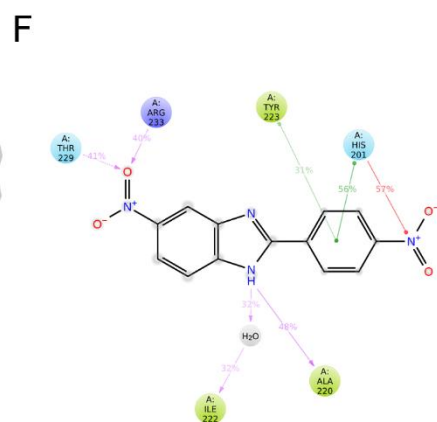
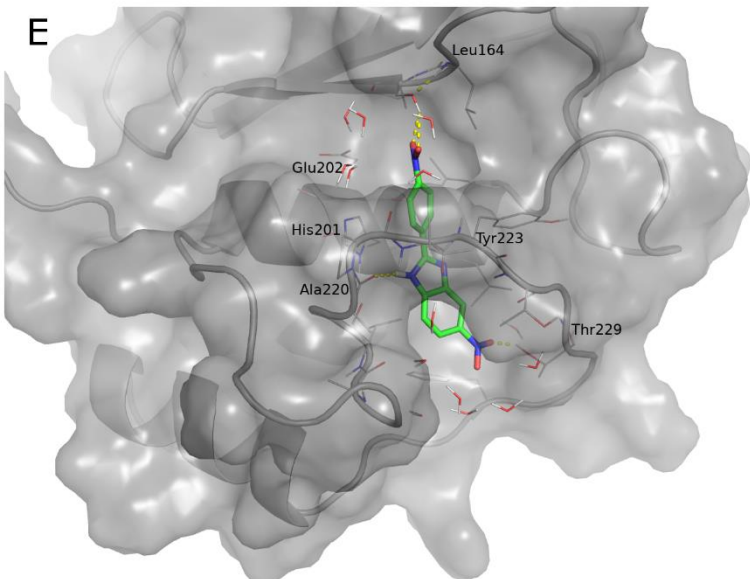
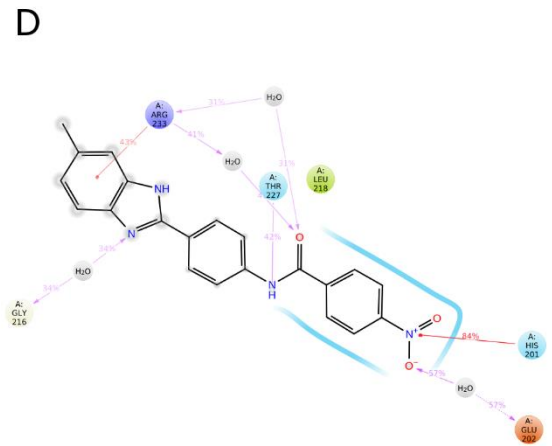
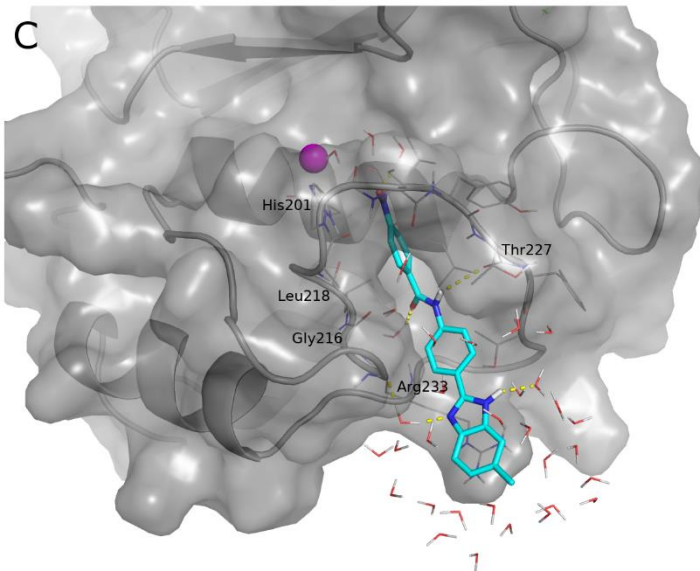
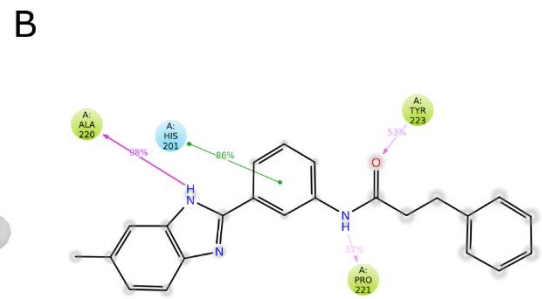
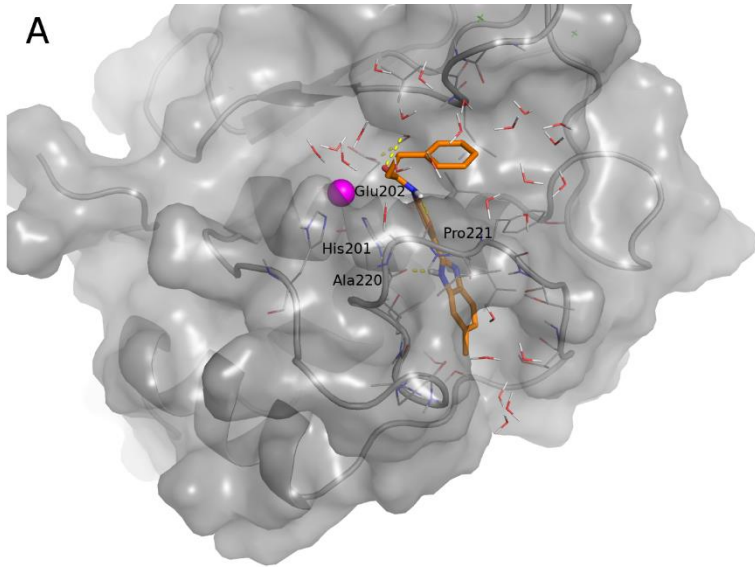


Figure 5. On the left the 3D complexes of MMP-2 (grey cartoon and solid surface) in complex with ligand **2** (A, cyan C atoms), **28** (C, orange C atoms), and **42** (E, green C atoms) as resulting from MD simulation (an average conformation is represented). Ligands are reported as sticks and H-bonds are represented as yellow dashed lines. For sake of clarity, only residues and water molecules at 4 Å from the ligand are represented as lines. On the right, the 2D representation of interactions between MMP-2 and ligand **2** (B), **28** (D) and **42** (F) retrieved in more than 30% of saved MD frames are depicted.

The inhibition mechanism of non-zinc binding inhibitors has been investigated in particular with respect to MMP-13 and results strongly relate to the possibility to exploit the diverse amino acid composition of MMP specificity loop, increasing selectivity [28, 31]. In fact, the large variability of the S1' loop sequence among MMPs influences both shape and flexibility of this pocket, allowing the opening of an accessory pocket in the case of MMP-13 and MMP-8. The occupancy of this transient pocket allowed to obtain very selective inhibitors. On the other hand, the relevance of protein dynamics in the MMP inhibition is a well-known issue: Fabre and coworkers collected several examples that underline the need to account for target flexibility in the search for MMP inhibitors [35]. With respect to non-zinc binding ligands, in particular, the role of dynamic effects seems to be particularly relevant even when no conformational rearrangement of the specificity loop is possible. As an example, in a previous work we attempted to rationalize activity data of two MMP-2 non-zinc binding inhibitors combining different computational approaches [39]. In that study, results from MD calculations suggest that more active ligand is able to stabilize the protein structure by increasing the number of protein intramolecular H-bonds, thus reducing the specificity loop fluctuations. It can be envisioned a similar mechanism also for the currently developed ligands. However, addressing this issue, i.e. designing ligands for a moving target, still remains a difficult goal.

3. Conclusions

In conclusion, starting from previously identified non-zinc-binding ligands, we setup a virtual screening campaign that allowed the identification of new inhibitors characterized by the phenylbenzimidazole scaffold. Starting from the selected **2** prototype, the synthesis of a large library of compounds brought us to disclose more effective MMP-2 inhibitors belonging to the non-zinc-binding class through a structure-based refinement process supported by LLE and LE correlation and computational studies.

Using MD simulations, we explored the binding process of most interesting ligands eliciting relevant interactions between the identified scaffold, providing useful suggestions for next optimization.

4. Experimental section

4.1. Chemical methods

All reagents were purchased from Sigma Aldrich Chemicals (Milan, Italy) and were used without purification. The reactions were monitored by TLC (silica gel, UV254) with UV light (short wave ultraviolet 254 nm and long wave ultraviolet 365 nm). All anhydrous reactions were performed under argon or nitrogen atmosphere. The column chromatography was performed using Fluka silica gel 60 Å (63-200 µm) or silica gel Si 60 (40-63 µm). Mass spectra were recorded on a HP MS 6890-5973 GC/MSD spectrometer, electron impact 70 eV, equipped with a HP ChemStation or with an Agilent 6530 Series Accurate-Mass Quadrupole Time-of-FLIGHT (Q-TOF) LC/MS; ¹H NMR and ¹³C NMR were recorded using the suitable deuterated solvent on a Varian Mercury 300 or 500 NMR Spectrometer. Chemical shifts (δ) are expressed as parts per million (ppm) and coupling constants (J) in Hertz (Hz). Melting points were determined in open capillaries on a Gallenkamp electrothermal apparatus and are uncorrected. Microanalyses of solid compounds were carried out with an Eurovector Euro EA 300 model analyser and were within ±0.4% of the theoretical values.

General procedure for the preparation of 2-arylbenzimidazoles and 2-arylbenzoxazoles.

Acyl chloride (2 mmol) was added to a solution of 1,2-diaminobenzene or 2-aminophenol (1 mmol) in anhydrous pyridine (20 ml) and the resulted mixture was heated to reflux overnight. The mixture was poured into an ice bath and the precipitate obtained was collected, washed with water and used for the next step without purification. The crude product was suspended in a mixture of *p*-toluene sulfonic acid monohydrate (1.6-2.0 mmol) and xylene (50 ml) and refluxed overnight.

For the synthesis of benzimidazoles derivatives, the reaction mixture was partitioned between EtOAc (100 ml) and 2 M HCl solution (100 ml) and the organic layer extracted twice with 2M HCl solution (100 ml). The combined aqueous layers were alkalized with 1 M NaOH solution until basic pH and extracted with EtOAc (3 X 100 ml). The combined organic layers were washed with brine, dried over anhydrous Na₂SO₄, filtrated and evaporated *in vacuo*.

For the synthesis of benzoxazole derivatives and for ester **34**, the reaction mixture was partitioned between EtOAc (100 ml) and NaHCO₃ solution (100 ml). The organic layer was washed with brine, dried over anhydrous Na₂SO₄, filtered and evaporated *in vacuo*.

The products were opportunely purified by crystallization or column chromatography.

6-bromo-2-phenyl-1H-benzo[d]imidazole (33): Brown solid, 34% yield; mp: 206-209 °C (CHCl₃/Hexane). ¹H NMR (500 MHz, [D₆] DMSO): δ = 3.00-3.60 (br, 1H, NH), 7.32 (dd, J = 8.79, J = 1.76, 1H, aromatic), 7.49-7.56 (m, 4H, aromatics), 7.76 (s, 1H, aromatic), 8.15 (d, J = 6.44, 2H, aromatics). GC-MS: m/z (%): 274 [M+ 2] (99), 272 [M] (100).

Methyl 4-(6-bromo-1H-benzo[d]imidazol-2-yl)benzoate (34): Brown solid, 52% yield; mp: 226-229 °C (CHCl₃). ¹H NMR (500 MHz, [D₆] DMSO): δ = 3.89 (s, 3H, CH₃), 7.36-7.38 (dd, J = 8.32, J = 1.96, 1H, aromatic), 7.59 (d, J = 8.32, 1H, aromatic), 7.82 (bs, 1H, aromatic), 8.12 (d, J = 8.56, 2H, aromatics), 8.30 (d, J = 8.56, 2H, aromatic), 13.00 (bs, 1H, NH). GC-MS: m/z (%): 332 [M+2] (96), 330 [M] (100), 301 (37), 299 (33), 273 (14), 271 (15).

6-bromo-2-(4-nitrophenyl)-1H-benzo[d]imidazole (37): Brown solid, 84% yield; mp: 254-249 °C (EtOAc/hexane). ¹H NMR (500 MHz, [D₆] DMSO): δ = 7.37-7.39 (dd, J = 8.81, J = 1.96, 1H, aromatic), 7.61 (d, J = 8.81, 1H, aromatic), 7.84 (d, J = 1.96, 1H, aromatic), 8.39-8.43 (m, 4H, aromatics), 13.25 (bs, 1H, NH). MS(ESI): m/z: 318 [M+2-H]⁻, 316 [M-H]⁻; MS²: m/z (%): 288 (100), 286 (96), 272 (26), 270 (26).

6-bromo-2-(3-nitrophenyl)-1H-benzo[d]imidazole (38): Brown solid, 85% yield; mp: 220-222 °C (Et₂O). ¹H NMR (500 MHz, [D₆] DMSO): δ = 7.38 (dd, J = 8.32, J = 1.96, 1H, aromatic), 7.60 (d, J = 8.81, 1H, aromatic), 7.83-7.87 (m, 2H, aromatics), 8.33-8.35 (m, 1H, aromatic), 8.60 (d, J = 8.81, 1H, aromatic), 8.99 (t, J = 1.96, 1H, aromatic), 13.00 (bs, 1H, NH). MS(ESI): m/z: 318 [M+2-H]⁻, 316 [M-H]⁻; MS²: m/z (%): 288 (80), 286 (67), 272 (72), 270 (38), 260 (100), 258 (62).

6-methyl-2-(4-nitrophenyl)-1H-benzo[d]imidazole (39): yellow solid, 61% yield; mp: 205-207 °C (EtOAc). ¹H NMR (300 MHz, CDCl₃): δ = 2.49 (s, 3H, CH₃), 7.15-7.46 (d, J = 8.2, 1H, aromatic), 7.42 (bs, 1H, aromatic), 7.57 (bs, 1H, aromatic), 8.20 (d, J = 8.79, 2H, aromatics), 8.30 (d, J = 8.79, 2H, aromatics), 9.76-10.70 (br, 1H, NH). MS(ESI): m/z: 252 [M-H]⁻; MS²: m/z (%): 222 (100), 206 (23), 276 [M + Na]⁺.

6-methyl-2-(3-nitrophenyl)-1H-benzo[d]imidazole (40): White solid, 78% yield; mp: 201-204 °C (EtOAc). ¹H NMR (500 MHz, CD₃OD): δ = 2.48 (s, 3H, CH₃), 4.86 (br (H₂O), 1H, NH), 7.15 (d, J = 8.32, 1H, aromatic), 7.41 (s, 1H, aromatic), 7.51 (d, J = 8.32, 1H, aromatic), 7.78 (t, J = 7.83, 1H, aromatic), 8.30-8.33 (m, 1H, aromatic), 8.43 (d, J = 7.83, 1H, aromatic), 8.94 (s, 1H, aromatic). MS(ESI): m/z: 252 [M-H]⁻; MS²: m/z (%): 222 (70), 206 (23), 194 (100).

2-(4-nitrophenyl)-1H-benzo[d]imidazole (41): Yellow solid, 43% yield; mp: > 250 °C (EtOAc). ¹H NMR (300 MHz, [D₆] DMSO): δ = 3.3 (bs, 1H, NH), 7.23-7.26 (m, 2H, aromatics), 7.65 (m, 2H, aromatics), 8.34-8.44 (m, 4H, aromatics). MS(ESI): m/z: 238 [M-H]⁻; MS²: m/z (%): 208 (100).

6-nitro-2-(4-nitrophenyl)-1H-benzo[d]imidazole (42): Yellow solid, 26% yield; mp: > 250 °C (MeOH). ¹H NMR (300 MHz, [D₆] DMSO): δ = 3.00-4.00 (br, 1H, NH), 7.80 (d, J = 9.08, 1H, aromatic), 8.13 (dd, J = 9.08, J = 1.76, 1H, aromatic), 8.40-8.43 (m, 4H, aromatics), 8.51 (d, J = 1.76, 1H, aromatic). GC-MS: m/z (%): 284 [M] (100), 254 (23), 238 (18), 208 (10), 192 (25).

2-(5-nitrofuranyl)-1H-benzo[d]imidazole (45): Yellow solid, 45% yield; mp: 228-230 °C (chromatography eluent: EtOAc/Hexane 8:2 v/v). ¹H NMR (500 MHz, [D₆] DMSO): δ = 7.28-7.30 (m, 2H, aromatics), 7.49 (d, J = 3.91, 1H, heteroaromatic), 7.6-7.7 (m, 2H, aromatics), 7.89 (d, J = 3.91, 1H, heteroaromatic), 13.48 (bs, 1H, NH). MS(ESI): m/z: 228 [M-H]⁻; MS²: m/z (%): 181 (100), 154 (38).

2-(3-nitrophenyl)-1H-benzo[d]imidazole (55): Grey solid, 70% yield. ¹H NMR (300 MHz, [D₆] DMSO): δ = 7.23 (m, 2H, aromatics), 7.58 (bs, 1H, aromatic), 7.68 (bs, 1H, aromatic), 7.81-7.86 (t, J = 7.87, 1H, aromatic), 8.29-8.30 (m, 1H, aromatic), 8.57-8.61 (m, 1H, aromatic), 8.80-9.00 (s, 1H, aromatic), 13.28 (bs, 1H, NH). MS(ESI): m/z: 238 [M-H]⁻; MS²: m/z (%): 208 (100).

7-methyl-2-(3-nitrophenyl)-1H-benzo[d]imidazole (56): Grey solid, 53% yield. ¹H NMR (300 MHz, [D₆] DMSO): δ = 2.58 (s, 3H, CH₃), 7.03 (d, J = 7.03, 1H, aromatic), 7.13 (t, J = 7.62, 1H, aromatic), 7.44 (bs, 1H, aromatic), 7.83 (t, J = 7.9, 1H, aromatic), 8.31 (d, J = 8.20, 1H, aromatic), 8.63 (d, J = 7.62, 1H, aromatic), 9.05 (s, 1H, aromatic), 13.04 (bs, 1H, NH). MS(ESI): m/z: 251.9 [M-H]⁻; MS²: m/z (%): 222 (93), 206 (58), 194 (100).

2-(4-nitrophenyl)benzo[d]oxazole (46): Grey solid, 34% yield; mp: > 250 °C (Hexane/CHCl₃). ¹H NMR (500 MHz, CDCl₃): δ = 7.43-7.46 (m, 2H, aromatics), 7.65 (dd, J = 7.34, J = 1.47, 1H, aromatic), 7.83 (dd, J = 7.34, J = 1.47, 1H, aromatic), 8.40 (d, J = 8.81, 2H, aromatics), 8.45 (d, J = 8.81, 2H, aromatics). GC-MS: m/z (%): 240 [M] (100), 210 (16), 194 (25), 182 (20).

6-methyl-2-(4-nitrophenyl)benzo[d]oxazole (52): light brown solid, 88% yield; mp: 201-204 °C (Hexane/AcOEt). ¹H NMR (500 MHz, CDCl₃): δ = 2.53 (s, 3H, CH₃), 7.23 (d, J = 8.08, 1H, aromatic), 7.43 (s, 1H, aromatic), 7.68 (d, J = 8.08, 1H, aromatic), 8.36-8.41 (m, 4H, aromatics). GC-MS: m/z (%): 254 [M] (100), 224 (15), 208 (29), 196 (11), 78 (11).

5-methyl-2-(4-nitrophenyl)benzo[d]oxazole (53): white solid, 67% yield; mp: 209-212 °C (Hexane/AcOEt). ¹H NMR (500 MHz, CDCl₃): δ = 2.5 (s, 3H, CH₃), 7.23 (d, 1H, aromatic), 7.48 (d, 1H, aromatic), 7.60 (s, 1H, aromatic), 8.36 (d, J = 8.80, 2H, aromatics), 8.40 (d, J = 8.80, 2H, aromatics). GC-MS: m/z (%): 254 [M] (100), 208 (28).

1-methyl-5-nitro-2-(4-nitrophenyl)-1H-benzo[d]imidazole and 1-methyl-6-nitro-2-(4-nitrophenyl)-1H-benzo[d]imidazole (43)

K₂CO₃ (0.28 mmol) was added to a solution of 6-nitro-2-(4-nitrophenyl)-1H-benzo[d]imidazole (**42**) (0.14 mmol) in anhydrous *N,N*-dimethylformamide (3 ml) and the mixture was stirred at room temperature for 3 h. CH₃I (1.45 mmol) was added and the mixture was stirred at room temperature overnight. The solvent was evaporated *in vacuo* and the residue was partitioned between EtOAc and H₂O. The organic layer was washed with brine, dried over anhydrous Na₂SO₄, filtrated, and evaporated under *vacuum* to give a brown solid. It was purified by chromatography on silica gel (eluent: EtOAc/Hexane 3:7 v/v) to give the desired product.

Yellow solid, 40% yield; mp: 209 °C (dec) (chromatography eluent: EtOAc/Hexane 3:7 v/v). ¹H NMR (300 MHz, [D₆] DMSO): δ = 4.00 (s, 3H, CH₃), 7.90-7.95 (m, 1H, aromatic), 8.17-8.28 (m, 2H, aromatics), 8.41-8.44 (m, 2H, aromatics), 8.63 (d, J = 1.76, 1H, aromatic), 8.74 (d, J = 2.34, 1H, aromatic). GC-MS: m/z (%): 298 [M] (100), 297 [M-H] (41).

Procedure for the preparation of 2-(4-nitrophenyl)benzo[d]thiazole (47)

4-nitrobenzaldehyde (1.76 mmol) was added to the solution of 2-aminothiophenol (1.6 mmol) in DMSO (4 ml) and the mixture was heated to reflux for 1 h. The mixture was poured into an ice bath and the precipitate obtained was collected and washed with water to give a crude product that was crystallized from MeOH to give the desired product.

Red solid, 75% yield; mp: 230-233°C (MeOH). ¹H NMR (500 MHz, [D₆] DMSO): δ = 7.54 (t, J = 7.58, 1H, aromatic), 7.61 (t, J = 7.58, 1H, aromatic), 8.15 (d, J = 7.83, 1H, aromatic), 8.23 (d, J = 8.32, 1H,

aromatic), 8.35-8.41 (m, 4H, aromatics). GC-MS: m/z (%): 256 (100), 226 (15), 210 (34), 209 (31), 198 (13), 139 (12).

General procedure for the preparation of *N*-Boc 2-arylbenzimidazoles (57-60)

Cs₂CO₃ (2 mmol) and di-tert-butyl dicarbonate (1.2-1.6 mmol) were added to the solution of 2-aryl benzimidazoles derivatives (1 mmol) in anhydrous CH₃CN (10 ml) and the resulting mixture was stirred at room temperature under argon for 4-12 h. The solvent was evaporated *in vacuo* and the residue was partitioned between EtOAc and H₂O and the layers were separated. The organic phase was washed with brine, dried over anhydrous Na₂SO₄, filtrated and evaporated under reduced pressure. The crude product was purified by chromatography on silica gel (eluent: EtOAc/Hexane 1:1 v/v).

***N*-Boc 5-methyl-2-(4-nitrophenyl)-1*H*-benzo[*d*]imidazole and *N*-Boc 6-methyl-2-(4-nitrophenyl)-1*H*-benzo[*d*]imidazole (57):** Brown oil, 95% yield. ¹H NMR (500 MHz, CDCl₃): δ = 1.47 (s, 9H, -(CH₃)₃), 1.49 (s, 9H, -(CH₃)₃), 2.52 (s, 3H, CH₃), 2.55 (s, 3H, CH₃), 7.24-7.28 (m, 2H, aromatics), 7.69 (d, J = 8.32, 1H, aromatic), 7.60 (d, J = 0.98, 1H, aromatic), 7.84-7.91 (m, 6H, aromatics), 8.33-8.36 (m, 4H, aromatics). MS(ESI): m/z: 376 [M+Na]⁺; MS² m/z (%): 320 (100). 252 [M-H-100]⁻ (100).

***N*-Boc 2-(4-nitrophenyl)-1*H*-benzo[*d*]imidazole (58):** Brown oil, 97% yield. ¹H NMR (500 MHz, [D₆] DMSO): δ = 1.38 (s, 9H, -(CH₃)₃), 7.43-7.48 (m, 2H, aromatics), 7.80 (d, J = 7.33, 1H, aromatic), 7.99-8.01 (m, 2H, aromatics), 8.04 (d, J = 7.83, 1H, aromatic), 8.35-7.37 (m, 2H, aromatics). MS(ESI): m/z: 238 [M-H-100]⁻.

***N*-Boc 2-(3-nitrophenyl)-1*H*-benzo[*d*]imidazole (59):** Brown oil, 94% yield. ¹H NMR (300 MHz, CDCl₃): δ = 1.48 (s, 9H, -(CH₃)₃), 7.41-7.45 (m, 2H, aromatics), 7.67 (t, J = 7.9, 1H, aromatic), 7.79-7.82 (m, 1H, aromatic), 8.01-8.08 (m, 2H, aromatics), 8.33-8.37 (m, 1H, aromatic), 8.53 (t, J = 1.93, 1H, aromatic). MS(ESI): m/z: 362 [M+Na]⁺; MS²: m/z (%): 306 (100). 238 [M-H-100]⁻. MS²: m/z (%): 208 (100), 180 (92).

***N*-Boc 7-methyl-2-(3-nitrophenyl)-1*H*-benzo[*d*]imidazole (60):** Brown oil, 96% yield. ¹H NMR (300 MHz, [D₆] DMSO): δ = 1.34 (s, 9H, -(CH₃)₃), 2.56 (s, 3H, CH₃), 7.22 (d, J = 7.03, 1H, aromatic), 7.34 (t, J = 7.62, 1H, aromatic), 7.76-7.86 (m, 2H, aromatics), 8.14-8.17 (dd, J = 7.62, J = 1.17, 1H, aromatic), 8.34-8.38 (d, J = 7.62, 1H, aromatic), 8.54 (t, J = 1.76, 1H, aromatic). MS(ESI): m/z: 252 [M-H-100]⁻; MS²: m/z (%): 222 (94), 206 (54), 194 (100).

General procedure for the preparing of *N*-Boc 2-(aminophenyl)-1*H*-benzo[*d*]imidazoles (61- 64)

5% or 10% Pd/C (0.23-0.36 mmol) was added to the solution of nitro derivatives **57-60** (1 mmol) in EtOH or EtOH/EtOAc (2:1 v/v) and the solution was hydrogenated at room temperature at a pressure of 3 bar for 12-24 h. The reaction mixture was filtrated through a Celite pad and the solvent was evaporated *in vacuo* to give the crude product which was purified by chromatography on silica gel (eluent: EtOAc/Hexane 2:8 → 1:1 v/v).

***N*-Boc 5-methyl-2-(4-aminophenyl)-1*H*-benzo[*d*]imidazole and *N*-Boc 6-methyl-2-(4-aminophenyl)-1*H*-benzo[*d*]imidazole (61):** White solid, 74% yield. ¹H NMR (500 MHz, CDCl₃): δ = 1.47 (s, 9H, -(CH₃)₃), 1.50 (s, 9H, -(CH₃)₃), 2.49 (s, 3H, CH₃), 2.52 (s, 3H, CH₃), 3.87 (s, 4H, NH₂), 6.73-6.75 (m, 4H, aromatics), 7.16-7.18 (m, 2H, aromatics), 7.44-7.48 (m, 4H, aromatics), 7.54 (d, J = 0.98, 1H, aromatic), 7.62 (d, J = 7.83, 1H, aromatic), 7.82 (d, J = 0.98, 1H, aromatic), 7.84 (d, J = 8.32, 1H, aromatic). MS(ESI): m/z: 346 [M+Na]⁺; MS²: m/z (%): 290 (100).

***N*-Boc 2-(4-aminophenyl)-1*H*-benzo[*d*]imidazole (62):** White solid, 45% yield. ¹H NMR (500 MHz, [D₆] DMSO): δ = 1.43 (s, 9H, -(CH₃)₃), 5.57 (s, 2H, NH₂), 6.61-6.65 (m, 2H, aromatics), 7.32-7.37 (m, 4H, aromatics), 7.64-7.67 (m, 1H, aromatic), 7.87-7.89 (m, 1H, aromatic). MS(ESI): m/z: 332 [M+ Na]⁺. MS²: m/z (%): 276 (100). 308 [M-H]⁻; MS²: m/z (%): 252 (93), 208 (90), 207 (100).

***N*-Boc 2-(3-aminophenyl)-1*H*-benzo[*d*]imidazole (63):** White solid, 76% yield. ¹H NMR (300 MHz, CDCl₃): δ = 1.42 (s, 9H, -(CH₃)₃), 2.5 (bs, 2H, NH₂), 6.76-6.80 (m, 1H, aromatic), 6.95-6.98 (m, 2H, aromatics), 7.19-7.26 (m, 1H, aromatic), 7.35-7.38 (m, 2H, aromatics), 7.76-7.79 (m, 1H, aromatic), 8.01-8.04 (m, 1H, aromatic). MS(ESI): m/z: 310 [M+H]⁺; MS²: m/z (%): 254 (100), 210 (20).

***N*-Boc 7-methyl-2-(3-aminophenyl)-1*H*-benzo[*d*]imidazole (64):** White solid, 54% yield. ¹H NMR (300 MHz, [D₆] DMSO): δ = 1.34 (s, 9H, -(CH₃)₃), 2.54 (s, 3H, CH₃), 5.26 (s, 2H, NH₂), 6.66-6.73 (m, 2H, aromatics), 6.79-6.80 (t, J = 2.07, 1H, aromatic), 7.08-7.18 (m, 2H, aromatics), 7.27 (t, J = 7.62, 1H, aromatic), 7.73 (d, J = 7.62, 1H, aromatic). MS(ESI): m/z: 346 [M+Na]⁺; MS²: m/z (%): 290 (100), 246 (90). 322 [M-H]⁻; MS²: m/z (%): 248 (29), 222 (100).

General procedure for the preparing of 2-(3 or 4 aminophenyl)-1*H* benzo[*d*]imidazoles (36, 44, 78, 79), benzoxazole (81) and benzothiazole (48).

Iron powder (3-4 mmol) and 6 N HCl solution (1 ml) were added to the solution of the nitro derivatives (1 mmol) in EtOH (5 ml) and the mixture was heated to reflux under nitrogen for 3-5 h. After cooling to room temperature, the suspension was diluted with EtOAc (20 ml); a solution of 6 M NaOH (20 ml) was added until basic pH and the layers were separated. The aqueous layer was extracted with AcOEt (2 X 20 ml) and the combined organic layers were washed with brine, dried over anhydrous Na₂SO₄, filtered and evaporated under *vacuum*. The crude product was purified by chromatography on silica gel (eluent: EtOAc/Hexane 6:4 v/v or CHCl₃/MeOH 9.5:0.5 v/v to 9:1 v/v) or triturated with diethyl ether.

6-bromo-2-(4-aminophenyl)-1H-benzo[d]imidazole (36): Red solid, 82% yield; mp: 235-228 °C (EtOAc). ¹H NMR (500 MHz, CH₃OD): δ = 4.86 (b (H₂O), 3H, NH, NH₂), 6.79 (d, J = 8.81, 2H, aromatics), 7.30 (d, J = 7.83, 1H, aromatic), 7.43 (d, J = 7.83, 1H, aromatic), 7.66 (s, 1H, aromatic), 7.81 (d, J = 8.81, 2H, aromatics). MS(ESI): m/z: 288 [M+2-H]⁻, 286 [M-H]⁻; MS²: m/z (%): 206 (100).

2-(4-aminophenyl)-1H-benzo[d]imidazol-6-amine (44): Orange solid, 20% yield; mp: 223-227 °C (Hexane). ¹H NMR (500 MHz, [D₆] DMSO): δ = 4.02 (br, 2H, NH₂), 5.44 (s, 2H, NH₂), 6.43-6.59 (m, 1H, aromatic), 6.58 (s, 1H, aromatic), 6.61 (d, J = 8.32, 2H, aromatics), 7.17 (d, J = 8.32, 1H, aromatic), 7.70 (d, J = 7.83, 2H, aromatics), 11.82 (s, 1H, NH). MS(ESI): m/z: 223 [M-H]⁻. 247 [M+Na]⁺.

2-(4-aminophenyl)-benzo[d]thiazole (48): Yellow solid, 63% yield; mp: 153-156 °C (chromatography eluent: EtOAc/Hexane 6:4 v/v). ¹H NMR (500 MHz, CDCl₃): δ = 4.00 (s, 2H, NH₂), 6.74-6.77 (m, 2H, aromatics), 7.33 (t, J = 7.34, 1H, aromatic), 7.45 (t, J = 7.34, 1H, aromatic), 7.85 (d, J = 7.34, 1H, aromatic), 7.90-7.93 (m, 2H, aromatics), 8.00-8.01 (d, J = 7.34, 1H, aromatic). GC-MS: m/z (%): 226 [M] (100), 108 (11).

6-bromo-2-(3-aminophenyl)-1H-benzo[d]imidazole (78): Red solid, 56% yield. ¹H NMR (500 MHz, [D₆] DMSO): δ = 5.31 (s, 2H, NH₂), 6.68 (d, 1H, aromatic), 7.30 (m, 2H, aromatics), 7.40 (d, J = 8.81, 1H, aromatic), 7.44 (d, J = 8.81, 1H, aromatic), 7.56 (d, J = 8.32, 1H, aromatic), 7.62 (s, 1H, aromatic), 7.80 (s, 1H, aromatic), 12.85 (s, 1H, NH). MS(ESI): m/z: 288 [M+2-H]⁻, 286[M-H]⁻.

2-(4-aminophenyl)-1H-benzo[d]imidazole (79): Brown solid, 95% yield. ¹H NMR (300 MHz, [D₆] DMSO): δ = 5.57 (s, 2H, NH₂), 6.64 (d, J = 8.79, 2H, aromatics), 7.07-7.11 (m, 2H, aromatics), 7.40 (bs, 1H, aromatic), 7.50 (bs, 1H, aromatic), 7.82 (d, J = 8.79, 2H, aromatics), 12.40 (s, 1H, NH). MS(ESI): m/z: 208 [M-H]⁻; MS²: m/z %: 180 (100). 232 [M+Na]⁺.

5-methyl-2-(4-aminophenyl)benzo[d]oxazole (81): Yellow solid, 37% yield. ¹H NMR (500 MHz, CDCl₃): δ = 2.46 (s, 3H, CH₃), 4.03 (bs, 2H, NH₂), 6.74- 6.76 (m, 2H, aromatics), 7.09 (dd, J = 8.32, J =

0.98, 1H, aromatic), 7.39 (d, J = 8.32, 1H, aromatic), 7.48 (d, J = 0.98, 1H, aromatic), 8.02- 8.05 (m, 2H, aromatics). GC-MS: m/z (%): 224 (100), 195 (6.9), 118 (12).

General procedure for the preparation of *N*-acyl derivatives

Triethylamine (2 mmol) was added to the solution of aniline derivatives (1 mmol) in anhydrous THF and the appropriate acyl chloride (1.1-2 mmol) was added at 0 °C. The resulting mixture was stirred at room temperature under nitrogen atmosphere for 3-12h, the eluent was evaporated *in vacuo*, the residue was partitioned between EtOAc and 2M NaOH solution. The combined organic layers were washed with NH₄Cl ss, brine, dried over anhydrous Na₂SO₄, filtered, and evaporated under reduced pressure. The residue was purified by chromatography on silica gel (eluent: Hexane/ EtOAc 8:2 → 6:4 v/v).

***N*-(3-(6-bromo-1H-benzo[*d*]imidazol-2-yl)phenyl)-3-phenylpropanamide (17):** White solid, 29% yield; mp: 204-207 °C (EtOAc). ¹H NMR (500 MHz, [D₆] DMSO): δ = 2.67 (t, J = 7.83, 2H, CH₂), 2.94 (t, J = 7.83, 2H, CH₂), 7.16-7.20 (m, 1H, aromatic), 7.26-7.32 (m, 4H, aromatics), 7.34 (dd, J = 8.81, J = 1.95, 1H, aromatic), 7.47 (t, J = 7.83, 1H, aromatic), 7.52-7.58 (m, 1H, aromatic), 7.65 (d, J = 7.83, 1H, aromatic), 7.78 (d, J = 7.83, 2H, aromatics), 8.52 (t, J = 1.71, 1H, aromatic), 10.14 (s, 1H, NH), 13.10 (s, 1H, NH). ¹³C NMR (125 MHz, [D₆] DMSO): δ 31.22, 38.39, 117.91, 121.24, 121.52, 125.31, 126.42, 128.71, 128.79, 129.84, 130.59, 140.27, 141.58, 152.97, 171.08. MS(ESI): m/z: 444 [M+Na+2]⁺, 442 [M+Na]⁺, 420 [M+2-H]⁻, 418 [M-H]⁻; MS²: m/z (%): 288 (66), 286 (100). Anal. calcd for C₂₂H₁₈N₃OBr*0.25H₂O: C 62.20%, H 4.39%, N 9.89%, found: C 62.32 %, H 4.30%, N 9.96%.

***N*-(4-(6-bromo-1H-benzo[*d*]imidazol-2-yl)phenyl)-3-phenylbutanamide (22):** Orange solid, 30% yield; mp: 209-216 °C (dec) (EtOAc). ¹H NMR (500 MHz, CD₃OD): δ = 2.00-2.06 (m, 2H, CH₂), 2.43 (t, J = 7.34, 2H, CH₂), 2.71 (t, J = 7.34, 2H, CH₂), 4.89 (b (CH₃OH), 2H, NH), 7.15-7.29 (m, 5H, aromatics), 7.36 (d, J = 8.32, 1H, aromatic), 7.50 (bs, 1H, aromatic), 7.65-7.75 (m, 1H, aromatic), 7.77 (d, J = 8.56, 2H, aromatics), 8.02 (d, J = 8.56, 2H, aromatics). ¹³C NMR (125 MHz, CD₃OD): δ 27.03, 34.87, 35.96, 115.09, 119.66, 124.29, 125.44, 125.57, 127.12, 128.01, 128.11, 140.94, 141.47, 152.91, 173.07. MS(ESI): m/z: 436 [M+2+H]⁺, 434 [M+H]⁺; MS² m/z (%): 290 (57), 288 (46). Anal. calcd for C₂₃H₂₀BrN₃O: C 63.60%, H 4.64%, N 9.67%, found: C 63.32 %, H 4.71%, N 9.52%.

***N*-(4-(1H-benzo[*d*]imidazol-2-yl)phenyl)-3-phenylpropanamide (23):** White solid, 18% yield; mp: 240 °C (dec) (chromatography eluent: EtOAc/Hexane 6:4 v/v). ¹H NMR (300 MHz, [D₆] DMSO): δ =

2.66 (t, J = 7.69, 2H, CH₂), 2.92 (t, J = 7.69, 2H, CH₂), 7.13-7.28 (m, 7H, aromatics), 7.39-7.53 (bs, 2H, aromatics), 7.72 (d, J = 8.78, 2H, aromatics), 8.06-8.09 (d, J = 8.78, 2H, aromatics), 10.14 (s, 1H, NH), 12.76 (bs, 1H, NH). MS(ESI): m/z: 340 [M-H]⁻; MS² m/z (%): 340 (100), 282(13), 208 (6). 364 [M+Na]⁺.

***N*-(4-(6-bromo-1*H*-benzo[*d*]imidazol-2-yl)phenyl)-4-nitrobenzamide (30):** Orange solid, 55% yield; mp: > 250 °C (AcOEt). ¹H NMR (500 MHz, [D₆] DMSO): δ = 7.30-7.32 (d, J = 8.32, 1H, aromatic), 7.52 (d, J = 8.32, 1H, aromatic), 7.75 (s, 1H, aromatic), 7.96 (d, J = 8.81, 2H, aromatics), 8.16-8.21 (m, 4H, aromatics), 8.38 (d, J = 8.81, 2H, aromatics), 10.81 (bs, 1H, NH), 12.94 (bs, 1H, NH). ¹³C NMR (125 MHz, [D₆] DMSO): δ 113.45, 114.26, 120.91, 121.47, 125.43, 125.70, 127.70, 129.75, 134.59, 140.81, 140.96, 145.85, 149.70, 152.58, 152.89, 164.58. MS(ESI): m/z: 437 [M+2-H]⁻, 435 [M-H]⁻; MS² m/z (%): 314 (100), 312 (87). Anal. calcd for C₂₃H₁₃N₄O₃Br*0.5H₂O: C 53.83 %, H 3.16%, N 12.55%, found: C 53.79 %, H 3.11%, N 12.27%.

***N*-(4-(6-bromo-1*H*-benzo[*d*]imidazol-2-yl)phenyl)benzamide (31):** Orange solid, 41% yield; mp: > 250 °C (EtOAc/MeOH). ¹H NMR (500 MHz, [D₆] DMSO): δ = 3.00-4.00 (br, 1H, NH), 7.30-7.32 (m, 1H, aromatic), 7.52-7.63 (m, 4H, aromatics), 7.75 (s, 1H, aromatic), 7.96-7.98 (m, 4H, aromatics), 8.15 (d, J = 8.81, 2H, aromatics), 10.50 (s, 1H, NH). ¹³C NMR (125 MHz, [D₆] DMSO): δ 113.42, 114.27, 120.73, 121.38, 125.19, 127.63, 128.20, 128.90, 132.21, 135.22, 141.49, 145.90, 152.90, 166.27. MS(ESI): m/z: 394 [M+2+H]⁺, 392 [M+H]⁺; MS² m/z (%): 291 (77), 289 (63), 210 (33), 105 (70). Anal. calcd for C₂₀H₁₄N₃OBr*0.5H₂O: C 59.87 %, H 3.77%, N 10.47%, found: C 60.27 %, H 3.80%, N 10.50%.

***N*-(4-(6-bromo-1*H*- benzo[*d*]imidazol-2-yl)phenyl)-3-phenylpropanamide (32):** White solid, 16% yield; mp: 246 °C (dec) (EtOAc). ¹H NMR (500 MHz, [D₆] DMSO): δ = 2.67 (t, J = 7.58, 2H, CH₂), 2.93 (t, J = 7.58, 2H, CH₂), 7.18 (t, 1H, J = 6.85, aromatic), 7.25-7.31 (m, 5H, aromatics), 7.51 (d, J = 8.32, 1H, aromatic), 7.75 (d, J = 8.32, 3H, aromatics), 8.08 (d, J = 8.32, 2H, aromatics), 10.17 (s, 1H, NH), 12.97 (s, 1H, NH). ¹³C NMR (125 MHz, [D₆] DMSO): δ 31.22, 38.39, 117.91, 121.24, 121.52, 125.54, 126.42, 128.71, 128.79, 129.84, 130.59, 140.27, 141.58, 152.97, 171.08. MS(ESI): m/z: 420 [M+2-H]⁻, 418 [M-H]⁻; MS² m/z (%): 362 (48), 360 (100), 285 (42). Anal. calcd for C₂₂H₁₈N₃OBr: C 62.87%, H 4.32%, N 10.00%, found: C 62.79 %, H 4.30%, N 9.98%.

***N*-(4-(benzo[*d*]thiazol-2-yl)phenyl)benzamide (49):** White solid, 67% yield; mp: > 236-239°C (CHCl₃). ¹H NMR (500 MHz, [D₆] DMSO): δ = 7.43-7.46 (m, 1H, aromatic), 7.52-7.57 (m, 3H,

aromatics), 7.61-7.63 (m, 1H, aromatic), 7.98-8.04 (m, 5H, aromatics), 8.10-8.15 (m, 3H, aromatics), 10.57 (s, 1H, NH). GC-MS: m/z (%): 330 (63), 105 (100), 77 (58).

***N*-(benzo[*d*]thiazol-2-yl)-4-nitrobenzamide (50):** Yellow solid, 56% yield; mp: > 250 °C (EtOH). ¹H NMR (500 MHz, [D₆] DMSO): δ = 7.35 (t, J = 7.58, 1H, aromatic), 7.48 (t, J = 7.58, 1H, aromatic), 7.77 (d, J = 7.83, 1H, aromatic), 8.02 (d, J = 7.83, 1H, aromatic), 8.34-8.39 (m, 4H, aromatics), 13.29 (bs, 1H, NH).

***N*-(6-chlorobenzo[*d*]thiazol-2-yl)-4-nitrobenzamide (51):** Orange solid, 20% yield; mp: > 250 °C (EtOH). ¹H NMR (500 MHz, [D₆] DMSO): δ = 7.47-7.50 (dd, J = 8.32, J = 1.96, 1H, aromatic), 7.76 (d, J = 8.32, 1H, aromatic), 8.15 (d, J = 1.96, 1H, aromatic), 8.33-8.38 (m, 4H, aromatics), 13.28 (bs, 1H, NH). GC-MS: m/z (%): 333 (27), 150 (100).

***N*-(4-(5-methylbenzo[*d*]oxazol-2-yl)phenyl)-4-nitrobenzamide (54):** Grey solid, 79% yield; mp: > 250 °C (AcOEt). ¹H NMR (500 MHz, [D₆] DMSO): δ = 2.43 (s, 3H, CH₃), 7.20-7.22 (d, J = 8.32, 1H, aromatic), 7.56 (s, 1H, aromatic), 7.62 (d, J = 8.32, 1H, aromatic), 8.02 (d, J = 8.81, 2H, aromatics), 8.18-8.21 (m, 4H, aromatics), 8.38 (d, J = 8.81, 2H, aromatics), 10.90 (bs, 1H, NH). ¹³C NMR (125 MHz, [D₆] DMSO): δ 21.46, 110.65, 119.90, 120.95, 122.33, 124.06, 126.72, 128.51, 129.81, 134.67, 140.70, 142.30, 142.38, 148.87, 149.76, 162.64, 164.77. Anal. calcd for C₂₁H₁₅N₃O₄: C 67.56 %, H 4.05%, N 11.25%, found: C 67.18 %, H 4.04%, N 11.01%.

***N*-Boc 2-(3-(3-phenylpropanamido)phenyl)-1*H*-benzo[*d*]imidazole (65):** White solid, 96% yield. ¹H NMR (300 MHz, [D₆] DMSO): δ = 1.32 (s, 9H, -(CH₃)₃), 2.64 (t, J = 7.62, 2H, CH₂), 2.90 (t, J = 7.62, 2H, CH₂), 7.12-7.31 (m, 6H, aromatics), 7.35-7.44 (m, 3H, aromatics), 7.63 (d, J = 8.2, 1H, aromatic), 7.72-7.75 (dd, J = 8.2, J = 1.17, 1H, aromatic), 7.96-7.99 (m, 2H, aromatics), 10.12 (s, 1H, NH). MS(ESI): m/z: 464 [M+Na]⁺; MS²: m/z (%): 408 (100), 364 (24). 440 [M-H]⁻; MS²: m/z (%): 340 (100).

***N*-Boc 7-methyl-2-(3-(3-phenylpropanamido)phenyl)-1*H*-benzo[*d*]imidazole (66):** White solid, 87% yield. ¹H NMR (300 MHz, [D₆] DMSO): δ = 1.31 (s, 9H, -(CH₃)₃), 2.55 (s, 3H, CH₃), 2.64 (t, J = 7.60, 2H, CH₂), 2.90 (t, J = 7.60, 2H, CH₂), 7.16-7.33 (m, 8H, aromatics), 7.38-7.43 (m, 1H, aromatic), 7.64-7.66 (m, 1H, aromatic), 7.78 (d, J = 8.52, 1H, aromatic), 7.95 (s, 1H, aromatic), 10.09 (s, 1H, NH). MS(ESI): m/z: 478 [M+Na]⁺; MS²: m/z (%): 422 (100), 378 (41). 454 [M-H]⁻; MS²: m/z (%): 354 (100).

***N*-Boc 7-methyl-2-(3-(4-phenylbutanamido)phenyl)-1*H*-benzo[*d*]imidazole (67):** White solid, 39% yield. ¹H NMR (300 MHz, [D₆] DMSO): δ = 1.80-1.92 (m, 2H, CH₂), 2.34 (t, J = 7.47, 2H, CH₂), 2.54

(s, 3H, CH₃), 2.60 (t, J = 7.47, 2H, CH₂), 7.00-7.34 (m, 8H, aromatics), 7.40 (t, J = 7.40, 1H, aromatic), 7.67 (d, J = 7.61, 1H, aromatic), 7.78 (d, J = 8.2, 1H, aromatic), 7.97 (s, 1H, aromatic), 10.15 (s, 1H, NH). MS(ESI): m/z: 468 [M-H]⁻; MS²: m/z (%): 368 [M-H-100]⁻ (100). 492 [M+Na]⁺; MS²: m/z (%): 436 (100), 392 (37).

N-Boc 2-(3-benzamidophenyl)-1H-benzo[d]imidazole (68): White solid, 51% yield. ¹H NMR (300 MHz, [D₆] DMSO): δ = 1.36 (s, 9H, -(CH₃)₃), 7.34-7.62 (m, 7H, aromatics), 7.75 (dd, J = 8.2, J = 1.17, 1H, aromatic), 7.90-8.00 (m, 4H, aromatics), 8.17 (s, 1H, aromatic), 10.42 (s, 1H, NH). MS(ESI): m/z: 436 [M+Na]⁺; MS²: m/z (%): 380 (100). 412 [M-H]⁻; MS²: m/z (%): 312 [M-H-100]⁻.

N-Boc 2-(3-(phenylsulfonamido)phenyl)-1H-benzo[d]imidazole (69): White solid, 38% yield. ¹H NMR (500 MHz, [D₆] DMSO): δ = 1.30 (s, 9H, -(CH₃)₃), 7.25-7.29 (m, 2H, aromatics), 7.33-7.45 (m, 4H, aromatics), 7.54 (t, J = 7.58, 2H, aromatics), 7.58-7.62 (m, 1H, aromatic), 7.74 (d, J = 7.34, 1H, aromatic), 7.79-7.81 (m, 2H, aromatics), 7.97 (d, J = 7.83, 1H, aromatic), 10.78 (bs, 1H, NH). MS(ESI): m/z: 472 [M+Na]⁺; MS²: m/z (%): 416 (100). 448 [M-H]⁻; MS²: m/z (%): 348 [M-H-100]⁻.

N-Boc 2-(3-(4-phenylbutanamido)phenyl)-1H-benzo[d]imidazole (70): White solid, 68% yield. ¹H NMR (300 MHz, [D₆]DMSO): δ = 1.33 (s, 9H, -(CH₃)₃), 1.85-1.91 (m, 2H, CH₂), 2.34 (t, J = 7.32, 2H, CH₂), 2.60 (t, J = 7.32, 2H, CH₂), 7.16-7.43 (m, 9H, aromatics), 7.62 (s, 1H, aromatic), 7.72-7.75 (m, 1H, aromatic), 7.95-7.99 (m, 1H, aromatic), 8.00 (s, 1H, aromatic), 10.06 (s, 1H, NH). MS(ESI): m/z: 454 [M-H]⁻; MS²: m/z (%): 354 [M-H-100] (100). 478 [M+Na]⁺; MS²: m/z (%): 422 (100).

N-Boc 2-(4-(4-phenylbutanamido)phenyl)-1H-benzo[d]imidazole (71): White solid, 50% yield. ¹H NMR (500 MHz, [D₆] DMSO): δ = 1.40 (s, 9H, (CH₃)₃), 1.80-1.96 (m, 2H, CH₂), 2.36 (t, J = 7.34, 2H, CH₂), 2.49 (t, J = 7.34, 2H, CH₂), 7.15-7.32 (m, 5H, aromatics), 7.35-7.42 (m, 2H, aromatics), 7.58-7.62 (m, 2H, aromatics), 7.70-7.75 (m, 3H, aromatics), 7.92-7.97 (m, 1H, aromatic), 10.11 (s, 1H, NH). MS(ESI): m/z: 454 [M-H]⁻; MS²: m/z (%): 354 [M-H-100] (100). 478 [M+Na]⁺; MS²: m/z (%): 422 (100).

N-Boc 2-(4-benzamidophenyl)-1H-benzo[d]imidazole (72): White solid, 76% yield. ¹H NMR (300 MHz, [D₆] DMSO): δ = 1.40 (s, 9H, -(CH₃)₃), 7.33-7.40 (m, 2H, aromatics), 7.51-7.74 (m, 6H, aromatics), 7.90-7.99 (m, 5H, aromatics), 10.46 (s, 1H, NH). MS(ESI): m/z: 436 [M+Na]⁺; MS²: m/z (%): 380 (100). 412 [M-H]⁻; MS²: m/z (%): 312 [M-H-100]⁻ (100).

N-Boc 2-(4-(4-bromobenzamido)phenyl)-1H-benzo[d]imidazole (73): White solid, 61% yield. ¹H NMR (500 MHz, CDCl₃): δ = 1.48 (s, 9H, -(CH₃)₃), 7.36-7.41 (m, 2H, aromatics), 7.63-7.68 (m, 4H,

aromatics), 7.75-7.78 (m, 5H, aromatics), 7.99 (s, 1H, NH), 8.02-8.03 (m, 1H, aromatic). MS(ESI): m/z: 494 [M+2+H]⁺, 492 [M+H]⁺; MS²: m/z %: 394 [M+2+H-100]⁺ (99), 392 [M+H-100]⁺ (74) .

***N*-Boc 5-methyl-2-(4-(3-phenylpropanamido)phenyl)-1*H*-benzo[*d*]imidazole and *N*-Boc 6-methyl-2-(4-(3-phenylpropanamido)phenyl)-1*H*-benzo[*d*]imidazole (74):** White solid, 59% yield. ¹H NMR (500 MHz, CDCl₃): δ = 1.44 (s, 9H, -(CH₃)₃), 1.46 (s, 9H, -(CH₃)₃), 2.50 (s, 3H, CH₃), 2.53 (s, 3H, CH₃), 2.98 (t, J = 7.83, 4H, CH₂), 3.09 (t, J = 7.83, 4H, CH₂), 7.10 (bs, 2H, NH₂), 7.18-7.34 (m, 13H, aromatics), 7.55-7.60 (m, 8H, aromatics), 7.65 (d, J = 8.32, 1H, aromatic), 7.88 (d, J = 8.32, 2H, aromatics). MS(ESI): m/z: 478 [M+23]⁺; MS²: m/z (%): 422 (100). 454 [M-H]⁻; MS²: m/z (%): 354 [M-H-100]⁻.

***N*-Boc 5-methyl-2-(4-(benzamido)phenyl)-1*H*-benzo[*d*]imidazole and *N*-Boc 6-methyl-2-(4-(benzamido)phenyl)-1*H*-benzo[*d*]imidazole (75):** White solid, 74% yield. ¹H NMR (500 MHz, CDCl₃): δ = 1.46 (s, 9H, -(CH₃)₃), 1.49 (s, 9H, -(CH₃)₃), 2.50 (s, 3H, CH₃), 2.54 (s, 3H, CH₃), 7.19-7.22 (m, 2H, aromatics), 7.53-7.69 (m, 12 H, aromatics), 7.78-7.81 (m, 4H, aromatics), 7.87-7.92 (m, 6H, aromatics), 7.98 (s, 2H, NH). MS(ESI): m/z: 450 [M+Na]⁺; MS²: m/z (%): 394 (100). 426 [M-H]⁻; MS²: m/z (%): 326 [M-H-100]⁻.

***N*-Boc 5-methyl-2-(4-(4-nitrobenzamido)phenyl)-1*H*-benzo[*d*]imidazole and *N*-Boc 6-methyl-2-(4-(4-nitrobenzamido)phenyl)-1*H*-benzo[*d*]imidazole (76):** Yellow solid, 69% yield. ¹H NMR (500 MHz, CDCl₃): δ = 1.48 (s, 9H, -(CH₃)₃), 1.50 (s, 9H, -(CH₃)₃), 2.50 (s, 3H, CH₃), 2.53 (s, 3H, CH₃), 7.21 (t, J = 7.09, 2H, aromatics), 7.54 (s, 1H, aromatic), 7.63-7.69 (m, 5H, aromatics), 7.77 (d, J = 8.32, 4H, aromatics), 7.86-7.89 (m, 2H, aromatics), 8.07 (d, J = 8.32, 4H, aromatics), 8.13 (s, 2H, NH), 8.35 (d, J = 8.32, 4H, aromatics). MS(ESI): m/z: 495 [M+Na]⁺; MS²: m/z (%): 439 (100). 471 [M-H]⁻; MS²: m/z (%): 371 [M-H-100]⁻ (100).

***N*-Boc 5-methyl-2-(4-(3-nitrobenzamido)phenyl)-1*H*-benzo[*d*]imidazole and *N*-Boc 6-methyl-2-(4-(3-nitrobenzamido)phenyl)-1*H*-benzo[*d*]imidazole (77):** Yellow solid, 73% yield. ¹H NMR (500 MHz, CDCl₃): δ = 1.46 (s, 9H, -(CH₃)₃), 1.48 (s, 9H, -(CH₃)₃), 2.48 (s, 3H, CH₃), 2.53 (s, 3H, CH₃), 7.17-7.21 (m, 2H, aromatics), 7.50 (s, 1H, aromatic), 7.60-7.71 (m, 7H, aromatics), 7.76 (d, J = 8.32, 4H, aromatics), 7.85-7.88 (m, 2H, aromatics), 8.26- 8.28 (m, 2H, aromatics), 8.33-8.39 (bs, 2H, NH), 8.39-8.41 (m, 2H, aromatics), 8.71- 8.73 (m, 2H, aromatics). MS(ESI): m/z: 473 [M+H]⁺; MS²: m/z (%): 373 (100).

General procedure for the deprotection of *N*-Boc acyl derivatives: obtainment of 14-16, 18-21, 24-29

Trifluoroacetic acid (TFA) (13 mmol) was added to the solution of *N*-Boc acyl derivatives (1 mmol) in dichloromethane (10 ml) and the solution was stirred at room temperature under nitrogen atmosphere for 2-12 h. The eluent was evaporated *in vacuo* and the residue was partitioned between EtOAc or CHCl₃ and 2N NaOH solution. The organic layer was washed with brine, dried over anhydrous Na₂SO₄, filtered and evaporated under *vacuum* to give the product which was crystallized with the opportune solvent or triturated with diethyl ether and filtered to afford the final compound.

***N*-(3-(1*H*-benzo[*d*]imidazol-2-yl)phenyl)-3-phenylpropanamide (14):** White solid, 43% yield; mp: 202- 205 °C (CHCl₃). ¹H NMR (300 MHz, [D₆] DMSO): δ = 2.66 (t, J = 7.75, 2H, CH₂), 2.94 (t, J = 7.75, 2H, CH₂), 7.16-7.20 (m, 3H, aromatics), 7.27-7.28 (m, 4H, aromatics), 7.44 (t, J = 7.9, 1H, aromatic), 7.55-7.59 (m, 2H, aromatics), 7.60-7.63 (m, 1H, aromatic), 7.78 (d, J = 8.2, 1H, aromatic), 8.5 (s, 1H, aromatic), 10.11 (bs, 1H, NH), 13.00 (bs, 1H, NH). MS(ESI): m/z: 340 [M-H]⁻; MS² m/z (%): 208 (100). 364 [M+Na]⁺.

***N*-(3-(7-methyl-1*H*-benzo[*d*]imidazol-2-yl)phenyl)3-phenylpropanamide (15):** White solid, 82% yield; mp: 212-216 °C (Et₂O). ¹H NMR (500 MHz, [D₆] DMSO): δ = 2.58 (s, 3H, CH₃), 2.68 (t, J = 4.70, 2H, CH₂), 2.95 (t, J = 4.70, 2H, CH₂), 6.98-7.00 (d, J = 4.11, 1H, aromatic), 7.06-7.11 (m, 1H, aromatic), 7.16-7.21 (m, 1H, aromatic), 7.24-7.36 (m, 5H, aromatics), 7.44-7.47 (m, 1H, aromatic), 7.66-7.90 (m, 2H, aromatics), 8.42 (s, 1H, aromatic), 10.25 (s, 1H, NH), 12.88 (s, 1H, NH). ¹³C NMR (125 MHz, [D₆] DMSO): δ 17.20, 17.64, 31.27, 38.42, 109.30, 117.73, 120.76, 121.27, 122.29, 122.88, 126.42, 128.71, 128.79, 129.73, 131.27, 140.22, 141.61, 150.72, 171.06. MS(ESI): m/z: 378 [M+Na]⁺; MS²: m/z (%): 201 (100). 354 [M-H]⁻; MS²: m/z (%): 222 (100). Anal. calcd for C₂₃H₂₁N₃O: C 77.72%, H 5.96%, N 11.82%, found: C 77.33%, H 5.98%, N 11.66%.

***N*-(3-(7-methyl-1*H*-benzo[*d*]imidazol-2-yl)phenyl)4-phenylbutanamide (16):** White solid, 30% yield; mp: 142-146 °C (CHCl₃/Hexane). ¹H NMR (500 MHz, [D₆] DMSO): δ = 1.91-1.96 (m, 2H, CH₂), 2.37 (t, J = 7.45, 2H, CH₂), 2.65 (t, J = 7.45, 2H, CH₂), 6.98 (d, J = 4.40, 1H, aromatic), 7.08 (t, J = 4.40, 1H, aromatic), 7.17-7.28 (m, 3H, aromatics), 7.29-7.31 (m, 2H, aromatics), 7.38 (d, J = 4.40, 1H, aromatic), 7.45 (t, J = 4.40, 1H, aromatic), 7.72 (d, J = 4.70, 1H, aromatic), 7.81-7.82 (d, J = 4.40, 1H, aromatic), 8.46 (s, 1H, aromatic), 10.12 (s, 1H, NH), 12.70 (bs, 1H, NH). ¹³C NMR (125 MHz, [D₆]

DMSO): δ 17.49, 27.22, 35.10, 36.24, 118.09, 120.84, 121.42, 122.64, 126.26, 128.77, 128.80, 129.60, 131.29, 140.25, 142.14, 171.62. MS(ESI): m/z: 368 [M-H]; MS²: m/z (%): 222 (100). Anal. calcd for C₂₄H₂₃N₃O: C 78.02%, H 6.27%, N 11.37%, found: C 77.88%, H 5.85%, N 11.17%.

***N*-(3-(1*H*-benzo[*d*]imidazol-2-yl)phenyl)benzamide (18):** White solid, 44% yield; mp: 129-132 °C (CHCl₃/ Hexane). ¹H NMR (300 MHz, [D₆] DMSO): δ = 7.19 (d, J = 5.27, 2H, aromatics), 7.49-7.63 (m, 6H, aromatics), 7.84-7.89 (m, 2H, aromatics), 7.99-8.02 (m, 2H, aromatics), 8.70 (s, 1H, aromatic), 10.43 (s, 1H, NH), 12.91 (bs, 1H, NH). MS(ESI): m/z: 336 [M+Na]⁺; MS² m/z: 337(100). 312 [M-H]⁻; MS² m/z (%): 234 (100).

***N*-(3-(1*H*-benzo[*d*]imidazol-2-yl)phenyl)benzenesulfonamide (19):** White solid, 52% yield; mp: 104-107 °C (CHCl₃/ Hexane). ¹H NMR (500 MHz, [D₆] DMSO): δ = 7.17-7.22 (m, 3H, aromatics), 7.39 (t, J = 8.07, 1H, aromatic), 7.50-7.61 (m, 4H, aromatics), 7.62-7.68 (m, 1H, aromatic), 7.76-7.81 (m, 3H, aromatics), 8.00 (t, J = 1.96, 1H, aromatic), 10.51 (bs, 1H, NH), 12.87 (s, 1H, NH). MS(ESI): m/z: 372 [M+Na]⁺. 348[M-H]⁻; MS² m/z: 207 (100).

***N*-(3-(1*H*-benzo[*d*]imidazol-2-yl)phenyl)-4-phenylbutanamide (20):** White solid, 82% yield; mp: 180-183 °C (Et₂O). ¹H NMR (300 MHz, [D₆] DMSO): δ = 1.86-1.96 (m, 2H, CH₂), 2.36 (t, J = 7.46, 2H, CH₂), 2.63 (t, J = 7.46, 2H, CH₂), 3.6 (bs, 1H, NH), 7.14-7.31 (m, 7H, aromatics), 7.46 (t, J = 7.9, 1H, aromatic), 7.56-7.64 (m, 3H, aromatics), 7.78 (d, J = 7.62, 1H, aromatic), 8.53 (s, 1H, aromatic), 10.09 (s, 1H, NH). MS(ESI): m/z: 378 [M+Na]⁺; MS² m/z (%): 356 (100), 177 (35). 354 [M-H]⁻; MS² m/z: 208 (100).

***N*-(4-(1*H*-benzo[*d*]imidazol-2-yl)phenyl)-4-phenylbutanamide (21):** White solid, 11% yield; 240 °C (dec) (CDCl₃). ¹H NMR (500 MHz, [D₆] DMSO): δ = 1.88-1.97 (m, 2H, CH₂), 2.36 (t, J = 7.09, 2H, CH₂), 2.63 (t, J = 7.09, 2H, CH₂), 7.17-7.31 (m, 7H, aromatics), 7.45-7.62 (m, 2H, aromatics), 7.74-7.76 (m, 2H, aromatics), 8.07-8.09 (m, 2H, aromatics), 10.11 (s, 1H, NH), 12.76 (s, 1H, NH). MS(ESI): m/z: 354 [M-H]⁻; MS² m/z: 208 (100).

***N*-(4-(1*H*-benzo[*d*]imidazol-2-yl)phenyl)benzamide (24):** White solid, 60% yield; mp: > 250°C (AcOEt). ¹H NMR (300 MHz, [D₆] DMSO): δ = 7.06-7.28 (m, 2H, aromatics), 7.48-7.67 (m, 5H, aromatics), 7.87-8.04 (m, 4H, aromatics), 8.15 (d, J = 8.79, 2H, aromatics), 10.45 (s, 1H, NH), 12.82 (bs, 1H, NH). MS(ESI): m/z: 336 [M+Na]⁺; MS²: m/z (%): 336 (100). 312 [M-H]⁻. MS²: m/z (%): 312 (18), 234 (100).

***N*-4-(1*H*-benzo[*d*]imidazol-2-yl)phenyl)-4-bromobenzamide (25):** White solid, 43% yield; mp: > 250 °C (AcOEt). ¹H NMR (500 MHz, [D₆] DMSO): δ = 3.80 (br, 1H, NH), 7.35-7.37 (m, 2H, aromatics), 7.68-7.70 (m, 2H, aromatics), 7.77 (d, J = 8.32, 2H, aromatics), 7.93 (d, J = 8.32, 2H, aromatics), 8.02 (d, J = 8.32, 2H, aromatics), 8.18 (d, J = 8.32, 2H, aromatics), 10.64 (bs, 1H, NH). MS(ESI): m/z: 394 [M+2+H]⁺, 392 [M+ H]⁺; MS²: 211 (100).

***N*-4-(6-methyl-1*H*-benzo[*d*]imidazol-2-yl)phenyl)-3-phenylpropanamide (26):** White solid, 59% yield; mp: > 250 °C (EtOAc). ¹H NMR (500 MHz, [D₆] DMSO): δ = 2.41 (s, 3H, CH₃), 2.67 (t, J = 7.58, 2H, CH₂), 2.93 (t, J = 7.58, 2H, CH₂), 6.99 (d, J = 7.83, 1H, aromatic), 7.17-7.33 (m, 6H, aromatics), 7.43 (d, J = 6.36, 1H, aromatic), 7.72 (d, J = 8.32, 2H, aromatics), 8.05 (d, J = 8.32, 2H, aromatics), 10.21 (s, 1H, NH), 12.63 (bs, 1H, NH). ¹³C NMR (125 MHz, [D₆] DMSO): δ 21.78, 31.20, 40.48, 119.47, 123.83, 125.28, 126.42, 127.42, 128.71, 128.79, 131.55, 140.99, 141.58, 151.30, 171.13. MS(ESI): m/z: 356 [M+H]⁺; MS²: m/z (%): 356 (96), 264 (25), 225 (46), 224 (100). 354 [M-H]⁻; MS²: m/z (%): 354 (55), 296 (21), 222 (50), 221 (100). Anal. calcd for C₂₃H₂₁N₃O*0.25H₂O: C 76.75 %, H 6.02%, N 11.67%, found: C 77.18%, H 5.86%, N 11.72%.

***N*-4-(6-methyl-1*H*-benzo[*d*]imidazol-2-yl)phenyl)benzamide (27):** White solid, 58% yield; mp: > 250 °C (EtOAc). ¹H-NMR (500 MHz, [D₆] DMSO): δ = 2.42 (s, 3H, CH₃), 6.8-7.04 (m, 1H, aromatic), 7.26-7.54 (m, 2H, aromatics), 7.55 (t, J = 7.34, 2H, aromatics), 7.61 (t, J = 7.34, 1H, aromatic), 7.94-7.98 (m, 4H, aromatics), 8.12 (d, J = 8.32, 2H, aromatics), 10.44 (s, 1H, NH), 12.65 (s, 1H, NH). GC-MS: m/z (%): 327 [M] (100), 105 (81), 77 (31).

***N*-4-(6-methyl-1*H*-benzo[*d*]imidazol-2-yl)phenyl)-4-nitrobenzamide (28):** Yellow solid, 49% yield; mp: > 250 °C (EtOH/H₂O). ¹H NMR (500 MHz, [D₆] DMSO): δ = 2.42 (s, 3H, CH₃), 7.01 (d, J = 7.34, 1H, aromatic), 7.35 (s, 1H, aromatic), 7.45 (d, J = 7.34, 1H, aromatic), 7.95 (d, J = 8.32, 2H, aromatics), 8.15 (d, J = 8.32, 2H, aromatics), 8.21 (d, J = 8.32, 2H, aromatics), 8.39 (d, J = 8.32, 2H, aromatics), 10.47 (bs, 1H, NH), 12.64 (bs, 1H, NH). ¹³C NMR (125 MHz, [D₆] DMSO): δ 21.80, 111.17, 111.38, 118.74, 118.90, 120.88, 123.62, 124.05, 126.46, 127.33, 129.73, 132.13, 135.71, 140.43, 140.88, 149.69, 150.99, 164.52. MS(ESI): m/z: 371[M-H]⁻; MS²: m/z (%): 248 (100). Anal. calcd for C₂₁H₁₆N₄O₃*0.5H₂O: C 66.13%, H 4.49%, N 14.69%, found: C 65.72%, H 4.31%, N 14.61%.

***N*-4-(6-methyl-1*H*-benzo[*d*]imidazol-2-yl)phenyl)-3-nitrobenzamide (29):** Yellow solid, 81% yield; mp: > 250 °C (AcOEt). ¹H NMR (500 MHz, [D₆] DMSO): δ = 2.41 (s, 3H, CH₃), 6.99 (d, J = 7.83, 1H, aromatic), 7.34 (s, 1H, aromatic), 7.44 (d, J = 6.85, 1H, aromatic), 7.83 (t, J = 7.83, 1H, aromatic), 7.95

(d, J = 8.32, 2H, aromatics), 8.15 (d, J = 8.32, 2H, aromatics), 8.42-8.46 (m, 2H, aromatics), 8.81 (s, 1H, aromatic), 10.8 (bs, 1H, NH), 12.6 (bs, 1H, NH). ¹³C NMR (125 MHz, [D₆] DMSO): δ 21.79, 111.42, 118.70, 120.97, 122.93, 123.62, 126.44, 126.76, 127.33, 130.70, 132.11, 134.70, 136.58, 140.42, 142.47, 148.24, 151.10, 163.96. MS(ESI): m/z: 373[M+H]⁺; MS²: m/z (%): 373 (62), 327 (52). Anal. calcd for C₂₁H₁₆N₄O₃: C 67.73%, H 4.33%, N 15.05%, found: C 67.45%, H 4.38%, N 14.92%.

General procedure for the preparation of benzoic acid derivatives **35** and **80**

14 ml of 1N NaOH solution was added to a solution of the corresponding ester (0.450 mmol) in 14 ml of THF and the system was stirred at room temperature for 4 h. The eluent was evaporated *in vacuo* and the residue was partitioned between CHCl₃ and H₂O, the aqueous layer was acidified to acid pH with 1N HCl solution and extracted with EtOAc (2 X 20 ml). The combined organic layers were washed with brine, dried over anhydrous Na₂SO₄, filtered, and the filtrate was evaporated under *vacuum* to give the desired product.

4-(6-bromo-1H-benzo[d]imidazol-2-yl)benzoic acid (35) White solid, 80% yield; ¹H NMR (500 MHz, [D₆] DMSO): δ = 3.41 (bs, 1H, OH), 7.37 (dd, J = 8.56, J = 1.71, 1H, aromatic), 7.5 (bs, 1H, aromatic), 7.80 (bs, 1H, aromatic), 8.10 (d, J = 6.85, 2H, aromatics), 8.27 (dd, J = 6.85, 2H, aromatics), 13.33 (bs, 1H, NH). ESI/MS: m/z (%): 317 [M+2-H]⁻, 315 [M-H]⁻; MS² m/z %: 273 (100), 271 (40).

3-(6-methyl-1H-benzo[d]imidazol-2-yl)benzoic acid (80): White solid, 42% yield. ¹H NMR (500 MHz, CD₃OD): δ = 2.49 (s, 3H, CH₃), 4.89 (b, NH, OH), 7.13 (d, J = 8.32, 1H, aromatic), 7.43 (s, 1H, aromatic), 7.51 (d, J = 8.32, 1H, aromatic), 7.66 (t, J = 7.83, 1H, aromatic), 8.14-8.16 (dd, J = 7.83, J₂ = 0.98, 1H, aromatic), 8.29 (d, J = 7.83, 1H, aromatic), 8.74 (d, J = 1.47, 1H, aromatic). ESI/MS: m/z: 251 [M-H]⁻; MS²: m/z %: 207 (100).

Preparation of 3-(6-methyl-1H-benzo[d]imidazol-2-yl)-N-phenethylbenzamide (13)

EDC (0.90 mmol), triethylamine (1.93 mmol) and HOBt (0.90 mmol) were added to the solution of acid compound **80** (0.5 mmol) in anhydrous *N,N*-dimethylformamide (5 ml) under nitrogen atmosphere). Phenethylamine (0.90 mmol) was added and, after 22 h, the mixture was poured into an ice bath; the precipitate obtained was collected and washed with water to give a crude product which was purified by chromatography on silica gel (eluent: EtOAc) and crystallized from EtOAc/Hexane.

White solid, 16% yield; mp: 184-186 °C (EtOAc/Hexane). ¹H NMR (500 MHz, [D₆] DMSO): δ = 2.42 (s, 3H, CH₃), 2.87 (t, J = 7.34, 2H, CH₂), 3.50-3.54 (m, 2H, CH₂), 7.02 (d, J = 7.82, 1H, aromatic), 7.17-7.21 (m, 1H, aromatic), 7.24-7.56 (m, 4H, aromatics), 7.30-7.47 (bs, 2H, aromatics), 7.60 (t, J = 7.83, 1H, aromatic), 7.85 (t, J = 7.83, 1H, aromatic), 8.21 (d, J = 7.83, 1H, aromatic), 8.62 (d, J = 1.47, 1H, aromatic), 8.76 (t, J = 5.62, 1H, NH), 12.91 (bs, 1H, NH). ¹³C NMR (125 MHz, [D₆] DMSO): δ 21.74, 35.55, 41.42, 111.59, 118.96, 123.84, 124.63, 125.81, 126.56, 128.45, 128.81, 129.11, 129.36, 130.94, 132.53, 135.90, 139.98, 142.37, 144.60, 150.64, 166.30. MS(ESI): m/z: 356 [M+H]⁺; MS²: m/z (%): 356 (100), 235 (52), 208 (75), 207 (98), 105 (72). Anal. calcd for C₂₃H₂₁N₃O*0.25H₂O: C 76.75 %, H 6.02%, N 11.67%, found: C 76.54 %, H 5.90%, N 11.57%.

4.2. Molecular modeling

Virtual screening

All calculations have been carried exploiting the Schrödinger Suite 2018_3 [44]. For the virtual screening campaign, a pharmacophore model has been generated using the structure of the 15 active compounds identified previously (see Table S1 of the SI). All ligands have been built in the Maestro graphical interface. The protonation state at pH 7.4 and possible tautomers were generated using the Ligand preparation routine in Maestro. The obtained structures were minimized to a derivative convergence of 0.05 kJ Å⁻¹ mol⁻¹ using the Polak–Ribiere conjugate gradient (PRCG) minimization algorithm, the OPLS3e force field, and the generalized Born/surface area (GB/SA) water solvation model implemented in MacroModel.

The Develop Pharmacophore Hypothesis module of Phase, has been used to generate the best common hypothesis. The 15 compounds have been divided into active (pIC₅₀ >4.5) and inactive compounds (pIC₅₀ <4.0). 100 conformers have been produced for each structure and hypothesis composed by five or six feature matching all active ligands were generated. The best obtained hypothesis was composed by five features.

For the virtual screening a library of virtual compounds from Asinex (610 542 compounds) was submitted to the REOS filter [40] and 493,175 resulting ligands passed to LigPrep calculation obtaining a final set of almost 1,300,000. These structures have been aligned to the Phase hypothesis after generating 50 conformers for each structure and saving compounds that matches 3 over 5 features. The top 10% ranking compounds have been submitted to docking in the MMP-2 structures obtained by MD

calculation as already reported [38]. Highest scored compounds have been visually inspected to verify the presence of the key interaction with the His201 imidazole ring. The final selection of virtual hits has been carried out through a consensus among the highest ranked in both pharmacophore screening and docking. Selected compounds have been purchased from Asinex.

Analogue selection.

A substructure search in the Asinex library has been carried out using the phenyl-benzimidazole as the scaffold. All available compounds containing this scaffold have been purchased along with a new batch of **1** that has been repurchased to confirm the activity and structure identity.

Docking of synthesized ligands

In order to rationalize the obtained results, docking calculations have been carried out for all synthesized ligands in the binding site of MMP-2, MMP-8, MMP-9 and MMP-13. Ligand structures have been built in Maestro and submitted to LigPrep calculation and Macromodel minimization as described before. Structure of studied proteins, selected through cross-docking calculations as previously reported [38], have been retrieved from the PDB (PDB ID: 1QIB, 3DNG, 4H1Q, 2OZR) and submitted to the Protein Preparation Wizard to fix bond orders, add hydrogen atoms, compute residue protonation states, optimize the H-bonding network, and relax the structure with a constrained minimization.

Glide Grid has been obtained for each protein using the default parameters and docking calculation have been carried out using both SP and XP setup.

Molecular Dynamics

Molecular dynamics calculations of the docked complexes of MMP-2 with **2**, **28** and **42** were carried out using Desmond implemented in the Schrodinger Suite 2018-3. Each complex was placed in a orthorombic box whose dimensions prevent self-interaction and then solvated by employing the single point charge (SPC) water model. Eleven sodium ions were added to ensure electrical neutrality. Parameters for the protein-ligand system were assigned using the OPLS3e forcefield. The final systems were constituted by 22 563, 22 541 and 22 565 for the three complexes with **2**, **28** and **42** respectively. A preliminary minimization of 2000 iterations to a convergence of 1 kcal/molÅ using the SD and LBFGS algorithms was carried out for each complex. The production phase of the simulation was forerun by six relaxation steps as by default, and lasted 20 ns, recording frames each 100 ps using a normal pressure temperature (NPT) ensemble with a Nosé-Hoover thermostat at 300 K and Martyna-Tobias-Klein

barostat at 1.01325 bar pressure. Smooth Particle Mesh Ewald method was also applied to analyze the electrostatic interactions with a cut-off distance set to 9.0 Å.

Trajectory analyses were carried out by using the and Maestro [44] graphical interfaces focusing on the root mean square deviation (RMSD) for the protein backbone, root mean square fluctuation (RMSF) of the residues to analyze the convergence of the structure to equilibrium, along with the ligand-protein interactions.

4.3. Biological methods

MMP inhibition assays

Catalytic domains of MMP-2, -8, -9 and -13 were purchased from Enzo Life Sciences. The assays were performed in triplicate in 96-well black microtiter plates (Corning, NBS). For assay measurements, inhibitor stock solutions (DMSO, 10 mM) were diluted to six different concentrations (1 nM–100 µM) in fluorometric assay buffer (50 mM Tris·HCl pH 7.5, 150 mM NaCl, 1 mM CaCl₂, 1 µM ZnCl₂, 0.05% Brij-35, and 1% DMSO). Enzyme and inhibitor solutions were incubated in the assay buffer for 15 min at room temperature before the addition of the fluorogenic substrate solution (OmniMMP[®]=Mca-Pro-Leu-Gly-Leu-Dpa-Ala-Arg-NH₂, Enzo Life Sciences, 2.5 µM final concentration or OmniMMP[®]RED=TQ3-GABA-Pro-Cha-Abu-Smc-His-Ala-Dab(6'-TAMRA)-Ala-Lys-NH₂, Enzo Life Sciences, 1 µM final concentration). After further incubation for 2–4 h at 37°C, fluorescence was measured (λ_{ex} =340 nm, λ_{em} =405 nm or λ_{ex} =545 nm, λ_{em} =572 nm) using a Perkin-Elmer Victor V3 plate reader. The MMP inhibition activity was expressed as percent inhibition and was calculated from control wells without inhibitor. IC₅₀ values were determined using GraphPad Prism version 5.0 software, and are expressed as mean ± SEM of at least three independent measurements in triplicate.

5. References

- [1] C.L. Chaffer, R.A. Weinberg, A perspective on cancer cell metastasis, *Science* 331 (2011) 1559-1564.
- [2] L.A. Liotta, K. Tryggvason, S. Garbisa, I. Hart, C.M. Foltz, S. Shafie, Metastatic potential correlates with enzymatic degradation of basement membrane collagen. *Nature* 284 (1980) 67-68.
- [3] H. Nagase, J.F. Woessner Jr, Matrix metalloproteinases, *J. Biol. Chem.* 274 (1999) 21491-21494.

- [4] L.M. Coussens, B. Fingleton, L.M. Matrisian, *Science* 295 (2002) 2387-2392.
- [5] J. Hu, P.E. Van den Steen, Q.A. Sang, G. Opdenakker, *Nat. Rev. Drug Discov.* 6 (2007) 480-498.
- [6] V.W. Yong, *Metalloproteinases: mediators of pathology and regeneration in the CNS*, *Nat. Rev. Neurosci.* 6 (2005) 931-944.
- [7] P.R. Brauer, *MMPs-role in cardiovascular development and disease*, *Front. Biosci.* 11 (2006) 447-478.
- [8] T. Klein, R. Bischoff, *Physiology and pathophysiology of matrix metalloproteases*, *Amino Acids* 41 (2011) 271- 290.
- [9] X.X. Wang, M.S. Tan, J.T. Yu, L. Tan, *Matrix metalloproteinases and their multiple roles in Alzheimer's disease*, *Biomed. Res. Int.* 2014 (2014) 908636.
- [10] T. Fischer, N. Senn, R. Riedl, *Design and structural evolution of matrix metalloproteinase inhibitors*, *Chem. Eur. J.* 25 (2019) 1-22.
- [11] M. Tauro, G. Shay, S.S. Sansil, A. Laghezza, P. Tortorella, A.M. Neuger, H. Soliman, C.C. Lynch, *Bone seeking matrix metalloproteinase-2 inhibitors prevent bone metastatic breast cancer growth*, *Mol. Cancer Ther.* 16 (2017) 494-505.
- [12] G.E. Terp, G. Cruciani, I.T. Christensen, F.S. Jørgensen, *Structural differences of matrix metalloproteinases with potential implications for inhibitor selectivity examined by the GRID/CPCA approach*, *J. Med. Chem.* 45 (2002) 2675-2684.
- [13] B. Pirard, *Insight into the structural determinants for selective inhibition of matrix metalloproteinases*, *Drug Discov. Today* 12 (2007) 640 - 646.
- [14] C.M. Overall, O. Kleifeld, *Towards third generation matrix metalloproteinase inhibitors for cancer therapy*, *Br. J. Cancer* 94 (2006) 941-946.
- [15] A. Dufour, C.M. Overall, *Missing the target: Matrix metalloproteinase antitargets in inflammation and cancer*, *Trends Pharmacol. Sci.* 34 (2013) 233-242.
- [16] E.I. Deryugina, J.P. Quigley, *Pleiotropic roles of matrix metalloproteinases in tumor angiogenesis: contrasting, overlapping and compensatory functions*, *Biochim. Biophys. Acta* 1803 (2010) 103-120.
- [17] R. Brauer, I.M. Beck, M. Roderfeld, E. Roeb, R. Sedlacek, *Matrix metalloproteinase-19 inhibits growth of endothelial cells by generating angiostatin-like fragments from plasminogen*, *BMC Biochem.* 12 (2011) 38.
- [18] R.E. Vandenbroucke, C. Libert, *Is there new hope for therapeutic matrix metalloproteinase inhibition?* *Nat. Rev. Drug Discov.* 13 (2014) 904-927.

- [19] C.M. Overall, O. Kleinfeld, Tumour microenvironment - opinion: validating matrix metalloproteinases as drug targets and anti-targets for cancer therapy, *Nat. Rev. Cancer* 6 (2006) 227-239.
- [20] A.H. Drummond, P. Beckett, P.D. Brown, E.A. Bone, A.H. Davidson, W.A. Galloway, A.J. Gearing, P. Huxley, D. Laber, M. McCourt, M. Whittaker, L.M. Wood, A. Wright, Preclinical and clinical studies of MMP inhibitors in cancer, *Ann. N. Y. Acad. Sci.* 878 (1999) 228-235.
- [21] J.A. Jacobsen, J.L.M Jourden, M.T. Miller, S.M. Cohen, To bind zinc or not to bind zinc: an examination of innovative approaches to improved metalloproteinase inhibition, *Biochim. Biophys. Acta*, 1803 (2010) 72-94.
- [22] C. Campestre, M. Agamennone, P. Tortorella, S. Preziuso, A. Biasone, E. Gavuzzo, G. Pochetti, F. Mazza, O. Hiller, H. Tschesche, V. Consalvi and C. Gallina, N-Hydroxyurea as zinc binding group in matrix metalloproteinase inhibition: Mode of binding in a complex with MMP-8, *Bioorg. Med. Chem. Lett.* 16 (2006) 20-24.
- [23] M. Tauro, A. Laghezza, F. Loiodice, M. Agamennone, C. Campestre, P. Tortorella, Arylamino methylene bisphosphonate derivatives as bone seeking matrix metalloproteinase inhibitors, *Bioorg. Med. Chem.* 21 (2013) 6456-6465.
- [24] M. Tauro, A. Laghezza, F. Loiodice, L. Piemontese, A. Caradonna, D. Capelli, R. Montanari, G. Pochetti, A. Di Pizio, M. Agamennone, C. Campestre, P. Tortorella, Catechol-based matrix metalloproteinase inhibitors with additional antioxidative activity, *J. Enzyme Inhib. Med. Chem.* 31 (2016) 25-37.
- [25] C. Campestre, M. Agamennone, M. Tauro, P. Tortorella, Phosphonate Emerging Zinc Binding Group in Matrix Metalloproteinase Inhibitors, *Curr. Drug Targets* 16 (2015) 1634-1644.
- [26] A. Di Pizio, M. Agamennone, A. Laghezza, F. Loiodice, P. Tortorella, Mimic catechins to develop selective MMP-2 inhibitors, *Monatshefte fuer Chemie* 149 (2018) 1293-1300.
- [27] A. Di Pizio, M. Agamennone, P. Tortorella, Non-zinc-binding inhibitors of MMP-13: GRID-based approaches to rationalize the binding process. *Curr. Topics Med. Chem.* 16 (2016) 449-459.
- [28] C.K. Engel, B. Pirard, S. Schimanski, R. Kirsch, J. Habermann, O. Klingler, V. Schlotte, K.U. Weithmann, K.U. Wendt, Structural basis for the highly selective inhibition of MMP-13, *Chem. Biol.* 12 (2005) 181-189.
- [29] A. Heim-Riether, S.J. Taylor, S. Liang, D.A. Gao, Z. Xiong, E. Michael August, B.K. Collins, B.T. Farmer II, K. Haverty, M. Hill-Drzewi, H.D. Junker, S. Mariana Margarit, N. Moss, T. Neumann, J.R.

- Proudfoot, L.S. Keenan, R. Sekul, Q. Zhang, J. Li, N.A. Farrow, Improving potency and selectivity of a new class of non-Zn-chelating MMP-13 inhibitors, *Bioorg. Med. Chem. Lett.* 19 (2009) 5321-5324.
- [30] C. Gege, B. Bao, H. Bluhm, J. Boer, B.M. Gallagher, B. Korniski, T.S. Powers, C. Steeneck, A.G. Taveras, V.M. Baragi. Discovery and evaluation of a non-Zn chelating, selective matrix metalloproteinase 13 (MMP-13) inhibitor for potential intra-articular treatment of osteoarthritis. *J. Med. Chem.* 55 (2012) 709-716.
- [31] T. Fischer, R. Riedl. Strategic targeting of multiple water-mediated interactions: a concise and rational structure-based design approach to potent and selective MMP-13 inhibitors. *ChemMedChem* 8 (2013) 1457-1461.
- [32] H. Nara, K. Sato, T. Naito, H. Mototani, H. Oki, Y. Yamamoto, H. Kuno, T. Santou, N. Kanzaki, J. Terauchi, O. Uchikawa, M. Kori, Discovery of Novel, Highly Potent, and Selective Quinazoline-2-carboxamide-Based Matrix Metalloproteinase (MMP)-13 Inhibitors without a Zinc Binding Group Using a Structure-Based Design Approach. *J. Med. Chem.* 57 (2014) 8886-8902.
- [33] G. Pochetti, R. Montanari, C. Gege, C. Chevrier, A.G. Taveras, F. Mazza, Extra binding region induced by non-zinc chelating inhibitors into the S1' subsite of matrix metalloproteinase 8 (MMP-8) *J. Med. Chem.* 52 (2009) 1040 -1049.
- [34] A.C. Dublanchet, P. Ducrot, C. Andrianjara, M. O'Gara, R. Morales, D. Compère, A. Denis, S. Blais, P. Cluzeau, K. Courté, J. Hamon, F. Moreau, M.L. Prunet, A. Tertre, Structure-based design and synthesis of novel non-zinc chelating MMP-12 inhibitors, *Bioorg. Med. Chem. Lett.* 15 (2005) 3787-3790.
- [35] B. Fabre, A. Ramos, B. de Pascual-Teresa, Targeting Matrix Metalloproteinases: Exploring the Dynamics of the S1' Pocket in the Design of Selective, Small Molecule Inhibitors. *J. Med. Chem.* 57 (2014) 10205-10219.
- [36] A. Di Pizio, A. Laghezza, P. Tortorella, M. Agamennone, Probing the S1' Site for the Identification of Non-Zinc-Binding MMP-2 Inhibitors. *ChemMedChem* 8 (2013) 1475–1482.
- [37] M. Agamennone, D.S. Belov, A. Laghezza, V.N. Ivanov, A.M. Novoselov, I.A. Andreev, N.K. Ratmanova, A. Altieri, P. Tortorella, A.V. Kurkin. Fragment-based discovery of 5-arylisatin based inhibitors of matrix metalloprotease-2 and 13, *ChemMedChem* 11 (2016) 1892-1898.
- [38] A. Ammazalorso, B. De Filippis, C. Campestre, A. Laghezza, A. Marrone, R. Amoroso, P. Tortorella, M. Agamennone, Seeking for non-zinc-binding MMP-2 inhibitors: synthesis, biological evaluation and molecular modelling studies, *Int. J. Mol. Sci.* 17 (2016) E1768.

- [39] A. Di Pizio, M. Agamennone, M. Aschi, An integrated computational approach to rationalize the activity of non-zinc-binding MMP-2 inhibitors, *PloS ONE* 7 (2012) e47774.
- [40] W.P. Walters, M.T. Sthal, M.A. Murcko, Virtual screening - an overview, *Drug Discov. Today* 3 (1998) 160-178.
- [41] L. Keurulainen, O. Salin, A. Siiskonen, J.M. Kern, J. Alvesalo, P. Kiuru, M. Maass, J. Yli-Kauhaluoma, P. Vuorela, Design and synthesis of 2-arylbenzimidazoles and evaluation of their inhibitory effect against chlamydia pneumonia, *J. Med. Chem.* 53 (2010) 7664-7674.
- [42] A.L. Hopkins, C.R. Groom, A. Alex, Ligand efficiency: a useful metric for lead selection. *Drug Discov. Today* 9 (2004) 430-431.
- [43] T.W. Johnson, R.A. Gallego, M.P. Edwards, Lipophilic efficiency as an important metric in drug design. *J. Med. Chem.* 61 (2018) 6401-6420.
- [44] Schrödinger Release, 2018-3: Maestro, Glide, LigPrep, MacroModel, Maestro, Phase, Desmond Molecular Dynamics System, D. E. Shaw Research, New York, NY, 2019. Maestro-Desmond Interoperability Tools, Schrodinger, LLC, New York, 2018.

Funding source

This work was supported by research funds from “G. d’Annunzio” University of Chieti-Pescara (MIUR, FAR 2017 grants to M. Agamennone).

Contributions

§AL and GL contributed equally to this work.

AC, AL and LP carried out the synthesis, analytical and spectroscopic characterization of the intermediates and target compounds. PT and FL supervised the synthesis. AL performed the enzyme inhibition tests. MA and ADP carried out the computational studies. GL wrote the paper. PT and MA supervised all the activities and together with GL wrote the paper.

Conflicts of interest

The authors declare no potential conflict of interest.